ACS OMEGA

Open Access

http://pubs.acs.org/journal/acsodf

Article

Exploring the Potential of PEG-Based Deep Eutectic Solvents as a Sustainable Alternative for Extraction of Biological Macromolecules Bovine Serum Hemoglobin

Masooma Siddiqui, Md Sayem Alam, and Maroof Ali*

Cite This: *ACS Omega* 2025, 10, 6839−6856

Read Online

ACCESS | Metrics & More | Article Recommendations | Supporting Information

ABSTRACT: In recent years, deep eutectic solvents (DESs) have garnered significant attention as promising green alternatives to conventional organic solvents for a wide range of applications. In this study, four novel polyethylene glycol (PEG)-based DESs were prepared and evaluated for their physicochemical properties, including density, dynamic viscosity, and kinematic viscosity. Fourier transform infrared spectroscopy (FT-IR) and NMR analyses revealed substantial intermolecular interactions between the hydrogen bond donor and hydrogen bond acceptor components, confirming the formation of stable DES systems. The application of the prepared DESs was tested in biological separation, specifically for the selective extraction of bovine serum hemoglobin (BHb). This study demonstrates the efficacy of PEG-based DESs in selectively extracting BHb. Among the DESs studied, DES-4 (PEG-600) achieved the highest extraction efficiency of 88%, while maintaining protein stability. Spectroscopic techniques, including UV−visible, fluorescence, dynamic light scattering, circular dichroism, and FT-IR, were employed to investigate the extraction mechanism, conformational changes in protein structure, and DES-protein interactions. These methods provided insights into the structural stability and functionality of BHb during the extraction process. The physicochemical characterizations confirmed the unique properties of PEG-based DESs, making them viable candidates for sustainable protein extraction. Their compatibility, excellent extraction efficiency, and short separation times underscore their potential as environmentally friendly and long-lasting substitutes for conventional separation techniques. This study highlights the advancement of DESs in green chemistry and biotechnological applications, offering an efficient and sustainable platform for protein extraction while maintaining structural integrity.

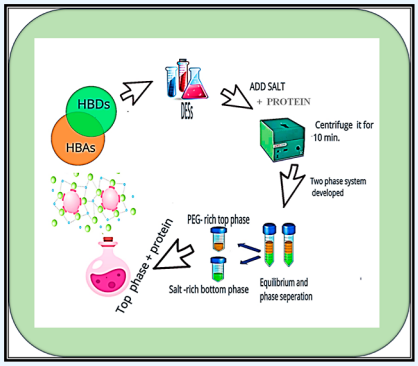

1. INTRODUCTION

In the realm of green chemistry, the development of sustainable and environmentally friendly alternatives to traditional solvents has become a pressing need, driven by concerns over environmental degradation and resource depletion.[1−3] Among the promising solutions, DESs have emerged as a novel class of green solvents with unique properties. DESs are formed by mixing a hydrogen bond donor (HBD) and a hydrogen bond acceptor (HBA), resulting in a eutectic mixture with a melting point significantly lower than that of its components.[4−6] This property not only broadens their application range but also simplifies their preparation, eliminating the need for complex synthesis routes and high-energy inputs. DESs are nontoxic, biodegradable, and cost-effective, making them ideal candidates for applications in sustainable extraction processes.[7−13] The extraction of biological macromolecules, particularly proteins, has been a focal area for DESs applications.[14,15] Proteins, as essential biomolecules, play a critical role in numerous fields, including biotechnology, pharmaceuticals, and food science. The ability to extract proteins efficiently while maintaining their structural integrity is pivotal for downstream applications. Conventional organic solvents, often used for such purposes, pose challenges due to their toxicity, environmental hazards, and high cost. DESs, by contrast, offer an environmentally friendly alternative that aligns with the principles of green chemistry.[16−21] PEG acts as an effective HBD, while its nontoxic and hydrophilic nature enhances the biocompatibility of the resulting DESs. In this study, we prepared four DESs by combining PEG with benzyl triethylammonium chloride (BTEAC), a commonly used HBA.[22−24] The 1:40 molar ratio was chosen based on optimization experiments, which indicated that this ratio provided the best balance of hydrogen bonding, viscosity, and phase separation efficiency. While the high PEG content might resemble a solute−solvent system, the formation of a hydrogen bond network, confirmed by FT-IR and NMR analyses, qualifies this as DESs. To further explore the potential of DESs

Received: October 7, 2024
Revised: January 25, 2025
Accepted: January 28, 2025
Published: February 14, 2025

in protein extraction, we employed biphasic systems. Biphasic systems consist of two immiscible liquid phases, such as DESs and aqueous salt solutions, that allow selective partitioning of biomolecules. This separation mechanism facilitates efficient protein extraction while reducing solvent waste. They offer a simple yet effective means for protein extraction, with the DES-rich phase selectively capturing target proteins.[25−27] The protein chosen for this study, bovine serum hemoglobin (BHb), serves as an ideal model for evaluating solvent−protein interactions. BHb is a globular protein with a heme group, widely studied for its structural and functional properties. Its extraction provides a model for evaluating solvent−protein interactions. This study aims to prepare and characterize PEG-based DESs, evaluate their performance in extracting BHb using an aqueous two-phase system (ATPS), and assess protein stability through spectroscopic techniques.[28,29] A range of advanced spectroscopic techniques was utilized to analyze the extraction process comprehensively. These included UV−visible spectroscopy for monitoring protein concentrations, 3D fluorescence spectroscopy for assessing protein structure and interactions, dynamic light scattering (DLS) for evaluating protein particle size distribution, circular dichroism (CD)[30,31] for determining secondary structural changes, and Fourier transform infrared spectroscopy (FT-IR) spectroscopy for identifying molecular interactions. This multipronged approach ensured a detailed evaluation of the DES-protein system, shedding light on the mechanisms underlying the extraction process. The findings of this study contribute significantly to the existing body of research on DESs, particularly in the context of protein extraction. By incorporating biphasic systems, this work not only enhances the efficiency and yield of the extraction process but also demonstrates the broader applicability of DESs as sustainable and cost-effective alternatives to conventional solvents. DESs' inherent properties, such as low toxicity, nonflammability, and reduced vapor pressure, further underscore their potential for large-scale applications in industries where solvent safety and sustainability are paramount. Moreover, this study highlights the advantages of PEG-based DESs over other solvent systems. Their ability to form stable hydrogen-bonded networks, coupled with their biocompatibility and low environmental impact, positions them as a transformative tool in green chemistry. The application of biphasic systems in DES-based extractions represents a significant advancement in the field, providing a platform for selective and efficient biomolecule recovery. Looking ahead, future research should focus on optimizing DES compositions to enhance their performance further, exploring their potential for extracting other biomolecules, such as carbohydrates, lipids, and nucleic acids. The integration of computational frameworks for DESs design could streamline the development of tailored solvents for specific applications, advancing their adoption across diverse fields, including food science, pharmaceuticals, and biotechnology.[32−38] Additionally, the environmental benefits of DESs, coupled with their cost-effectiveness, make them an attractive alternative for sustainable extraction processes on an industrial scale. Overall, the preparation and characterization of PEG-based DESs, combined with their application in biphasic systems for BHb extraction, underscore the potential of these green solvents to revolutionize traditional extraction methodologies.[39−41] This study serves as a foundation for further exploration of DESs in sustainable chemistry, offering insights into their design, functionality, and application in biomolecule recovery.

2. EXPERIMENT DIVISION

2.1. Chemicals Required. Benzyl triethylammonium chloride (≥98%purity), PEG200 (≥99%purity), PEG300 (≥99%purity), PEG400 (≥99%purity), and PEG600 (≥99% purity) were purchased from Sigma-Aldrich, USA, in the highest purity possible. Analytical-grade sodium carbonate (Na_2CO_3) (≥99.5% purity) was used without further purification. BHb (≥98%purity) was purchased from Acros Organics, and all the materials were used without further purification.

2.2. Synthesis of DESs. DESs were synthesized by mixing benzyl triethylammonium chloride (BTEAC) and polyethylene glycol (200, 300, 400, 600) at a defined molar ratio (1:40) (Figure 1). The 1:40 molar ratio of BTEAC to PEG was

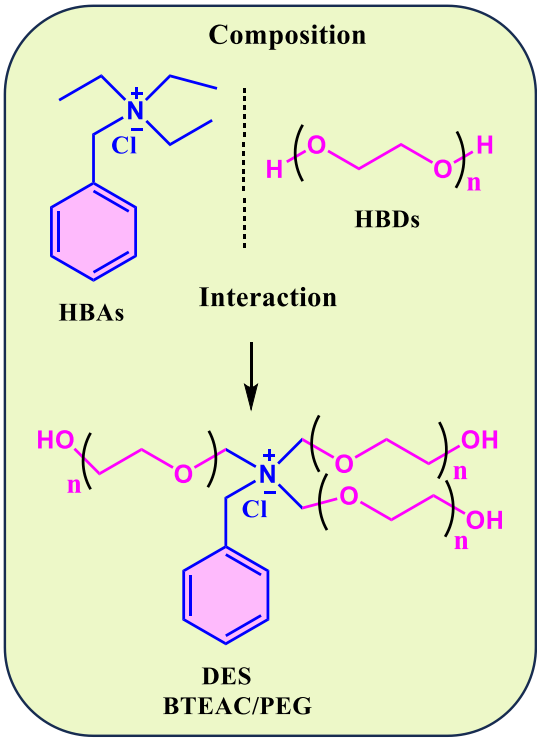

Figure 1. Chemical structures of HBAs, HBDs, and the proposed interaction of DESs are components are shown.

chosen based on optimization studies that demonstrated maximal hydrogen bonding and efficient phase separation at this ratio. This composition also resulted in DESs with suitable viscosity and density for protein extraction in an ATPS. The continuous stirring while heating to 80 °C for 1 h at air pressure results in a stable homogeneous liquid. All of the prepared DESs were dried for up to 3 h at 60 °C in a vacuum oven. The synthesized DESs were maintained in a desiccator and kept in sealed laboratory vials. The composition of HBA and HBD is shown in Table 1.

2.3. Characterization. A range of analytical techniques was employed to confirm their structural integrity and evaluate their physical properties. FT-IR and nuclear magnetic resonance (NMR) spectroscopy were utilized to elucidate the molecular structure of the DESs, ensuring the successful synthesis of the desired compounds. Additionally, UV,

https://doi.org/10.1021/acsomega.4c09125
ACS Omega 2025, 10, 6839−6856

Table 1. Basic Composition of DESs is Mentioned These Are as Follows

HBA	HBD	DESs	abbreviation	molar ratio
benzyl triethyl ammonium chloride (BTEAC)				
	polyethylene glycol 200	BTEAC/PEG-2	DES-1	1:40
	polyethylene glycol 300	BTEAC/PEG-3	DES-2	1:40
	polyethylene glycol 400	BTEAC/PEG-4	DES-3	1:40
	polyethylene glycol 600	BTEAC/PEG-6	DES-4	1:40

fluorescence spectroscopy was employed to assess the optical properties of the DESs. The physical characteristics, including density and viscosity, were measured to determine the suitability of the DESs for protein extraction applications. For the extraction study, various techniques, including UV spectroscopy, CD spectroscopy, 3D fluorescence spectroscopy, and DLS, were utilized to investigate structural changes and interactions within the DES−Na_2CO_3−BHb system. These comprehensive characterization results provide valuable insights into the efficiency and mechanism of the extraction process. Detailed information regarding the characterization methods and findings can be found in the Supporting Information (S2) section of this paper.

2.4. Protein Extraction Experiment. In this study, a novel DES-based protein extraction method was employed using BHb as the target protein. BHb samples were prepared by dissolving 20 mg of BHb in 10 mL of phosphate-buffered saline (PBS, pH 7.4). The DESs phase was preheated to 40 °C before mixing with the protein solution at a 1:1 (v/v) ratio. All experiments were performed in triplicate. The extraction process began with the preparation of a DES in a sodium salt (Na_2CO_3) solution. Specifically, a concentration of 0.6 g/mL of Na_2CO_3 solution was used as a salting-out agent to facilitate phase separation in the ATPS. The ratio of Na_2CO_3 solution to DESs was maintained at 1:1 (v/v), optimized for efficient separation and maximum protein recovery. Creating a system designated as (DES−Na_2CO_3−BHb) system. Following the addition of the protein, the mixture was subjected to centrifugation at 2400 rpm for 10 min. This centrifugation step facilitated the formation of a biphasic system, allowing for the separation of the DES-rich phase from the protein solution. After centrifugation, the DES-rich phase was carefully collected for further analysis and study of the extraction system. Route shows DES-based ATPS for the extraction of proteins (Figure 2). This method highlights the efficiency of using DES for protein extraction while maintaining the integrity of the target protein. The extraction efficiency (E) was calculated using the following equation

$$E\ \% = \frac{C_t V_t}{C_t V_t + C_b V_b}$$

separation coefficients (D) of the protein

$$(D) = \frac{C_t}{C_b}$$

$$\text{phase volume ratio } (R) = \frac{V_t}{V_b}$$

Where C_t and C_b are concentrations of the proteins in the DES-rich top phase and phosphate-rich bottom phase, respectively. V_t and V_b stand for the volume of the top phase and bottom phase, respectively. V_t and V_b were calculated by dividing the number of centimeters of the top phase and bottom phase by 1 mL volume.

3. RESULT AND DISCUSSION

3.1. Characterization of DESs. *3.1.1. NMR Analysis.* From Figure 3, the observed chemical shift values in parts per million (ppm) for nuclear magnetic resonance (NMR) peaks give the following information about the organic compounds. The presence of a peak at 0.74 ppm indicates the potential existence of a methyl group or a simple alkane. Moving into the range of 3.11−3.37 ppm, the aliphatic hydrogens may be associated with functional groups such as alcohols or amines. Notably, the signal at 3.65 ppm suggests a proton in a distinct chemical environment, possibly in proximity to an oxygen atom. The chemical shifts between 3.75 and 4.19 ppm indicate aliphatic hydrogens with varying local environments, hinting at the presence of different structural moieties. A distinct peak at 4.38 ppm further supports the presence of aliphatic hydrogens. The signals at 7.07−7.29 ppm fall within the typical range for aromatic hydrogens, suggesting the existence of an aromatic ring in the compound.[42,43] The peak at 3.65 ppm corresponds to the $-CH_2$ groups in PEG, while the peak at 7.09 ppm is attributed to aromatic protons of the benzyl group in BTEAC. Downfield shifts in these peaks confirm hydrogen bond interactions, highlighting the formation of a DES.

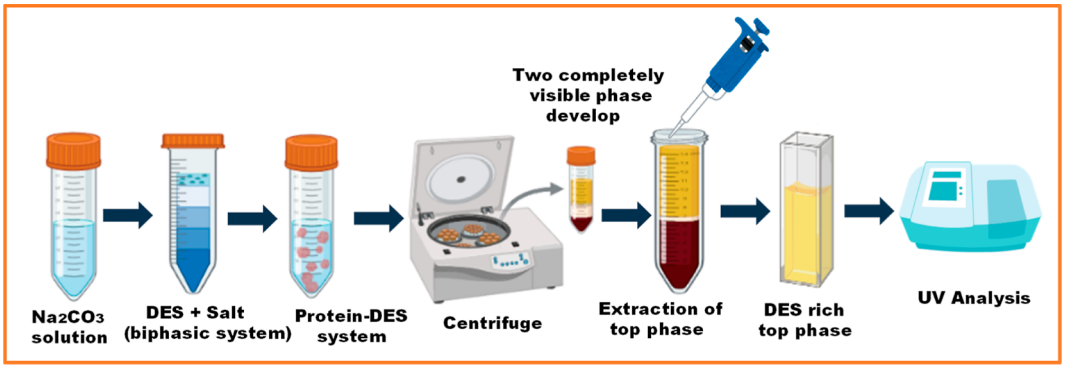

Figure 2. Route shows DES-based ATPS for the extraction of proteins.

https://doi.org/10.1021/acsomega.4c09125
ACS Omega 2025, 10, 6839−6856

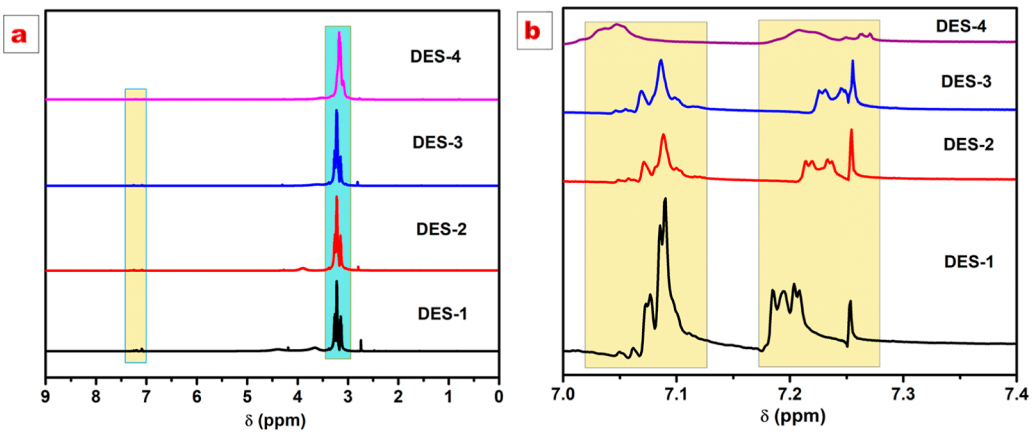

Figure 3. (a) NMR spectra of four prepared DES in Chloroform-D and (b) NMR spectra of the typical range for aromatic hydrogens, which confirm the component and structure of synthesized DESs.

3.1.2. FT-IR Analysis. The intermolecular interaction of the components in the synthesized DESs was verified using FT-IR. There are two peaks at 700 to 790 cm^{-1}, which show the alkenes or aromatic ring systems, and a sharp peak at 2950 to 3000 cm^{-1}. In (Figure 4), all DESs, n(OH) were at 3150 cm^{-1}

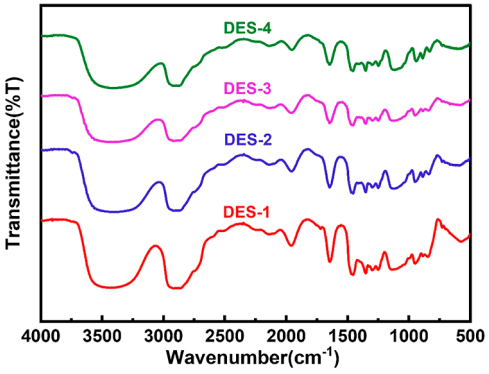

Figure 4. FT-IR spectra of the four prepared PEG-based DESs, highlighting characteristic functional groups and interactions indicative of hydrogen bonding and DES formation.

and had a broad peak attributed to the association of the hydroxyl group produced by hydrogen bonding. This shows the formation of hydrogen bonds with chlorine molecules.[44] And the shifting in I.R. frequency of three distinct oscillation modes, i.e., at ν1, 3010 to 3029 cm^{-1}; ν2, 1724 to 1741 cm^{-1}; and ν3, 3156 to 3124 cm^{-1} shown the formation of N−Cl bond.[45] An asymmetric "doublet" with medium intensity around 1370 cm^{-1} is characteristic of an isopropyl group, while an asymmetric "doublet" between 1365 and 1390 cm^{-1} is often due to an ethylene−OH group. The O−H-stretching modes from polyalcohols are mostly broad and very strong (3200−3650 cm^{-1}).[46]

3.2. Physicochemical Properties. The different physicochemical properties, such as density, viscosity, solubility, etc., are of utmost importance. Furthermore, the application of DESs depends on the physiochemical properties. Therefore, physicochemical properties of DESs, including solubility, viscosity, and density, are studied, and the results are presented here. Based on solubility, we can tell whether the above-synthesized DESs are hydrophobic or hydrophilic. To check the solubility, we took 2 mL of water and 2 g of DESs at room temperature, DESs with water after shaking up, and sonicated it for 10 min. DESs were utterly miscible in the water; this shows that all prepared DESs are hydrophilic. And further checked the solubility of prepared DESs in a nonpolar solvent. For this, benzene and toluene solutions are taken, and the same test condition is performed. All four DESs were miscible to it.

3.2.1. Density. 3.2.1.1. Density Variance of DESs on Temperature. The density (ρ) (g cm^{-3}) of all polyalcohol-based DESs was recorded at different temperatures. This has significance on the mass transfer and extraction ability of the medium. The highest density recorded in DESs-4 was 1.21 g cm^{-3} (BTEAC/PY), and the lowest was at 1.086 g cm^{-3} for DES-3 (BTEAC/PH) at 10% dilution. The density behavior of DESs deviates slightly from linearity with temperature due to the interplay of hydrogen bonding, ionic interactions, and molecular structuring unique to DESs. Similar trends have been observed in other DES studies, indicating that such effects are characteristic of DESs systems rather than measurement inconsistencies. At room temperature, the density decreased in the following order: DES-4 > DES-2 > DES-1 > DES-3. Thus, there is a significant relationship between the molecular weight and density of the DESs under investigation. Figure 5 shows the variation of density with temperature. Further fitting the data of Figure 5 with the

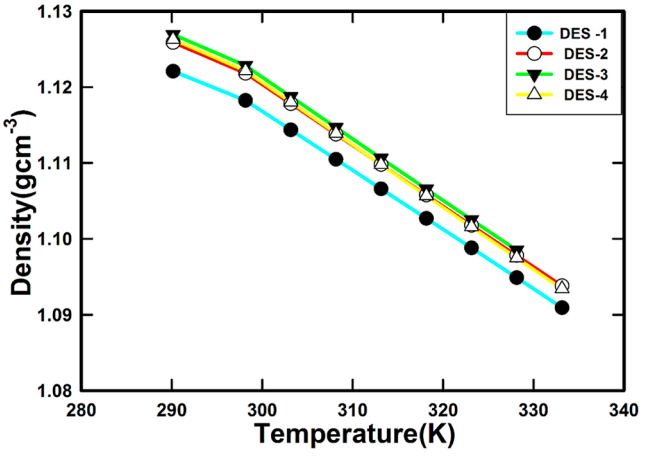

Figure 5. Variation of density for four synthesized DESs at different temperatures (290−350 K).

https://doi.org/10.1021/acsomega.4c09125
ACS Omega 2025, 10, 6839−6856

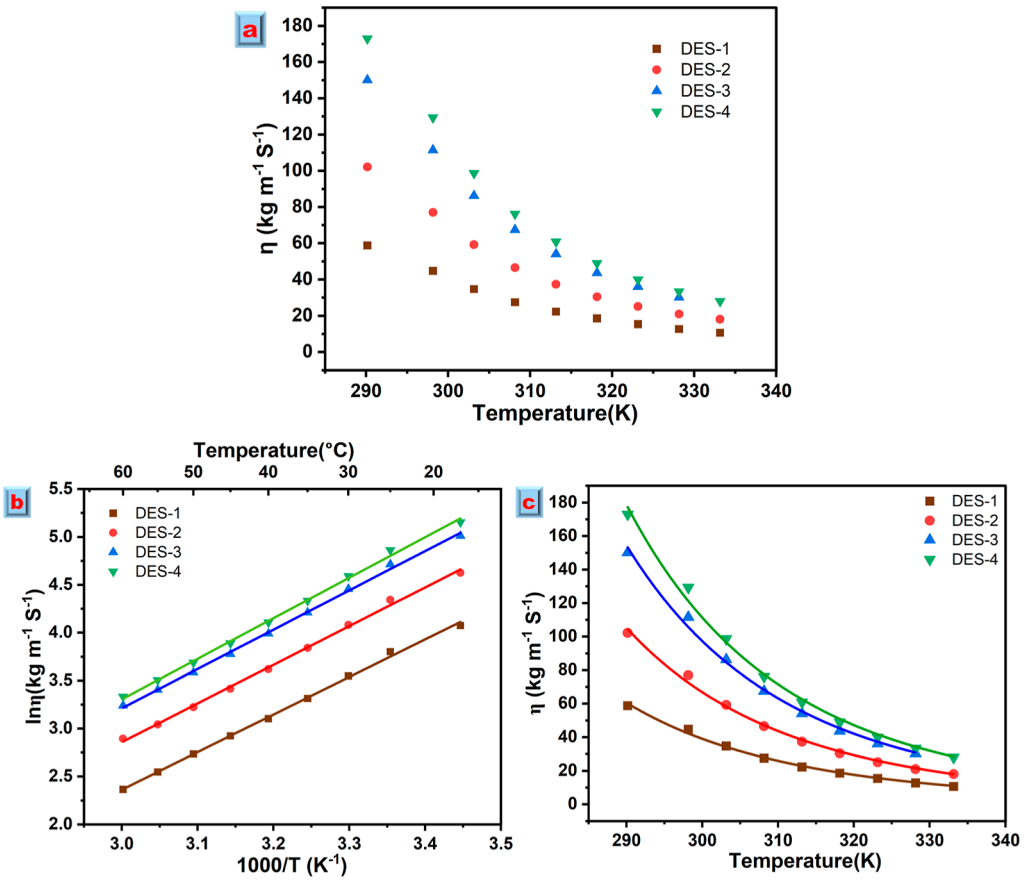

Figure 6. (a) Variation of dynamic viscosity for four synthesized DESs at different temperatures (290−350 K), (b) temperature dependence of dynamic viscosity fitted to the Arrhenius equation, and (c) temperature dependence of dynamic viscosity fitted to the VFT equation, highlighting the nonlinear decrease in viscosity with temperature.

variation of density with temperature, and the corresponding curve is fitted by equation $f = y0 + a \times x$ is shown in (Figure S2 and Table S1).

3.2.2. Dynamic Viscosity. 3.2.2.1. Temperature-Dependent Variation of Viscosity in DESs. The viscosity (η) (kg m^{-1} S^{-1}) of the synthesized DESs was measured, and it was discovered that the combination of HBD has a significant influence on its viscosity. The highest measured viscosity was 5.18 kg m^{-1} S^{-1} (DES-4), and the lowest was 4.22 kg m^{-1} S^{-1} (DES-3) at 293.15 K. The relationship between viscosity and temperature is reverse exponential. At room temperature, the sample's viscosity follows the same order as its density DES-4 > DES-2 > DES-1> DES-3. This could be due to the close interaction of the HBD's long-chain moiety with the HBA, which increases noncovalent interactions and, thus, viscosity on the medium under study. Temperature does not appear to have much influence on the sample's order of viscosity. Figure 6 shows the variation of dynamic viscosity with temperature. Further fitting the data of Figure 6, the variation of viscosity with temperature, and the corresponding curve is fitted by the equation $f = a \times \exp(-b \times x)$ is shown in (Figure S3 and Table S2) to show the variation of dynamic viscosity with temperature. And then again Arrehenius and Vogel−Fulcher−Tammann (VFT) fitting is done to analyze the viscosity trend.

3.2.2.2. Arrhenius Fitting. Dynamic viscosity data fitted to the Arrhenius equation (Figure 6b) reveal distinct trends influenced by the molecular weight of PEG in the synthesized DES systems. DES-1, composed of PEG-200 (low molecular weight), exhibits the lowest activation energy among the systems (Table S3), indicating that its viscosity is less sensitive to temperature changes. This is attributed to the shorter PEG chains in DES-1, which likely result in reduced intermolecular interactions and a more fluid system. The increase in activation energy with PEG molecular weight underscores the tunability of DES properties. DES-1 and DES-2, with lower Ea, are suitable for applications requiring lower viscosity and minimal temperature sensitivity. In contrast, DES-3 and DES-4, with higher Ea, are better suited for processes where viscosity stability over temperature fluctuations is desirable. The excellent fit of the Arrhenius model across all DESs, as reflected in high R^2 (~0.998) and Pearson's r, validates the data reliability and highlights the systematic correlation between molecular weight and viscosity behavior. This trend provides a foundation for tailoring DES compositions for specific industrial and scientific applications.

3.2.2.3. Vogel−Fulcher−Tammann. Further viscosity data is fitted with the VFT equation—y = pow(10, $A + B/(x - x0)$); (Figure 6c). Based on the VFT fitting results (Table S4), it is clear that as the molecular weight of PEG increases (from DES-1 with PEG-200 to DES-4 with PEG-600), the temperature sensitivity of the viscosity increases as well. DES-1 (PEG-200) shows the least sensitivity to temperature, while DES-4 (PEG-600) demonstrates the strongest temperature dependence. The minor shifts in the model parameters ×0 indicate similar behavior across all DES systems, with DES-4 showing a slight deviation from ideal behavior. However, all DES systems

https://doi.org/10.1021/acsomega.4c09125
ACS Omega 2025, 10, 6839−6856

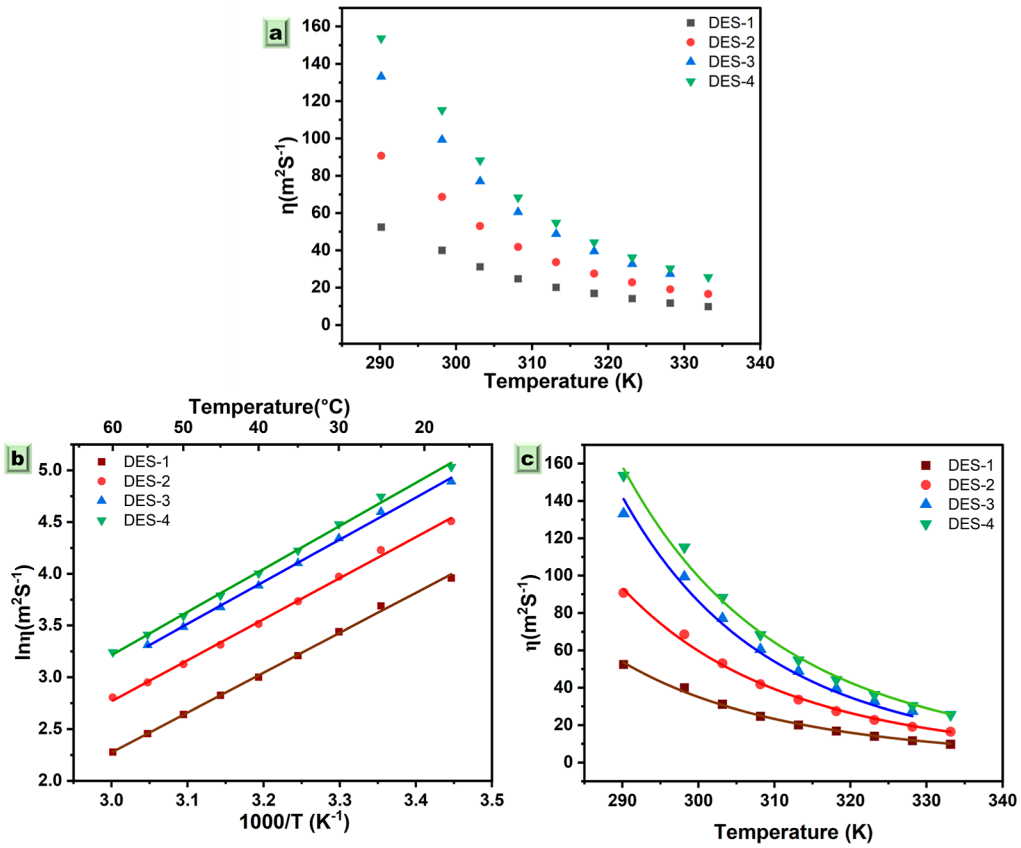

Figure 7. (a) Variation of kinematic viscosity for four synthesized DESs as a function of temperature (290−350 K), (b) temperature dependence of kinematic viscosity fitted to the Arrhenius equation, and (c) temperature dependence of kinematic viscosity fitted to the VFT equation, highlighting the nonlinear decrease in viscosity with temperature.

show excellent fits to the VFT model, with high *R*-squared values, suggesting that the VFT equation is an appropriate model for describing the viscosity−temperature relationship of these DESs.

3.2.3. Kinematic Viscosity. 3.2.3.1. Temperature-Dependent Variation of Kinematic Viscosity in DESs. The kinematic viscosity (m^2 S^{-1}) of the synthesized DESs was measured. It measures a fluid's internal resistance to flow under gravitational force.[47] It is calculated by dividing dynamic viscosity by density at the same temperature. And it follows the same pattern as dynamic viscosity. The highest one is observed in DES-4, and the lowest one is observed in DES-3. With the given sequence DES-4 > DES-2 > DES-1 > DES-3. Figure 7a shows the variation of kinematic viscosity with temperature. Further fitting the data of Figure 7a with the variation of kinematic viscosity with temperature, and the corresponding curve is fitted by the equation $f = a \times \exp(-b \times x)$ is shown in (Figure S4 and Table S5) to show the variation of kinematic viscosity with temperature. And then again Arrehenius and VFT fitting is done to analyze the viscosity trend.

3.2.3.2. Arrhenius Fitting. Kinematic viscosity data fitted to the Arrhenius equation (Figure 7b) reveal the same trend as dynamic viscosity (Table S6). The increasing molecular weight of PEG leads to longer polymer chains, which enhance hydrogen bonding and van der Waals interactions within the DES matrix. This creates more structured and viscous systems, requiring higher energy to overcome the resistance to flow. The trend highlights a direct correlation between the PEG molecular weight and the temperature sensitivity of the DESs' viscosity. DES-4 demonstrates the highest reflecting its stronger molecular interactions and higher structural rigidity. Such a progression emphasizes the tunability of DES properties based on the choice of PEG molecular weight, allowing tailored applications where viscosity control under temperature variation is critical. This systematic variation in activation energy provides valuable insights into designing DESs for specific industrial and scientific purposes.

3.2.3.3. VFT fitting. The VFT model (Figure 7c) adequately describes the temperature-dependent kinematic viscosity behavior of all four DES systems (Table S7), with high *R*-squared and adjusted *R*-squared values indicating good fits for the most part. As the PEG molecular weight increases from DES-1 to DES-4, the temperature sensitivity increases, which is reflected in the higher molecular weight DESs exhibiting stronger changes in viscosity with temperature. However, DES-4, with PEG-600, shows some deviation from the ideal fit, as evidenced by the higher reduced chi-square and lower *R*-squared values. Despite this, all DES systems display strong correlations, and the VFT model proves effective for analyzing the kinematic viscosity behavior of these solvents across a range of temperatures.

3.2.4. Fluorescence Spectroscopy. To assess the polarity of the synthesized DESs, fluorescence spectroscopy was conducted using various fluorescent dye probes, including ANS, pyrene, PCHO, coumarin 12, and Nile red. This technique allows for the observation of how these probes respond to variations in solvent dipolarity through their fluorescence emissions as shown in Figure 8. By measuring the maximum excitation wavelength (λex max) of the dyes in each DES, we were able to determine the relative polarity of the solvents. The

https://doi.org/10.1021/acsomega.4c09125
ACS Omega 2025, 10, 6839−6856

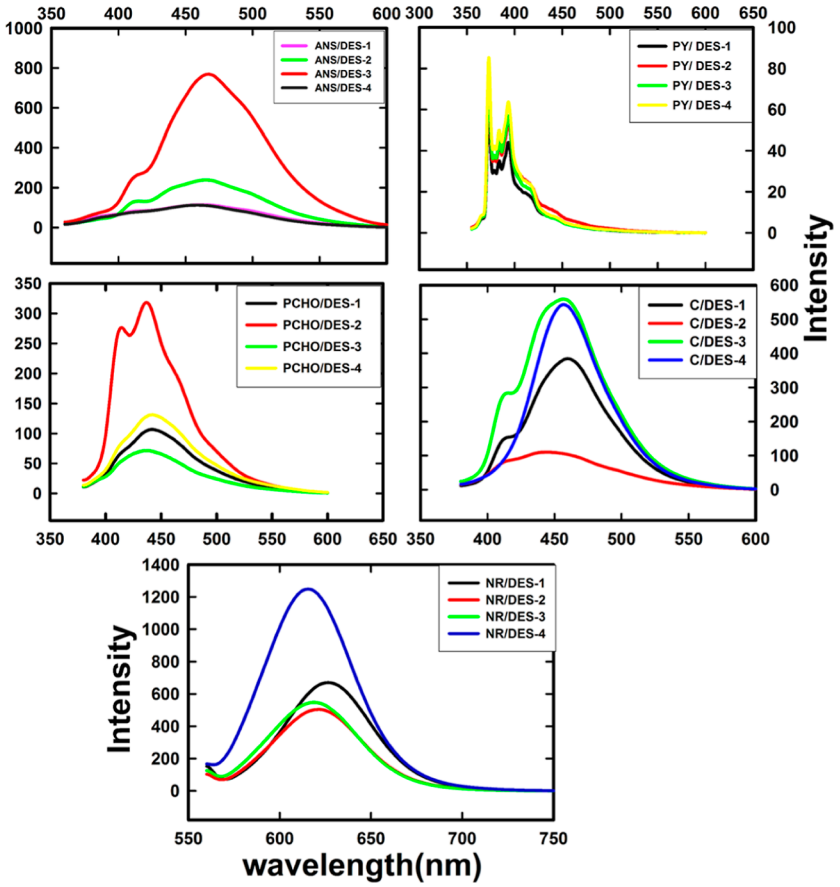

Figure 8. Fluorescence emission spectra of 8-anilino-1-naphthalenesulfonic acid (ANS, 10 mM, λex = 345 nm), Pyrene (PY, 10 mM, λex = 340 nm), PCHO (PCHO, 10 mM, λex = 365) Coumarin (C, 10 mM, λex = 457 nm) and Nile red (NR, 10 mM, λex = 590) in four DESs.

maximum excitation wavelengths (λex max) for each dye in the different DESs were measured and are summarized in the following table: The results revealed a distinct order of polarity among the four synthesized DESs, with the findings indicating that DES-1 exhibited the highest polarity, followed by DES-3, DES-2, and finally DES-4. The ANS probe showed the highest λex max in DES-1 at 468 nm, while the Nile red probe displayed the highest λex max in the same solvent at 626 nm all values are given in Table 2. This ranking was derived from the

Table 2. Fluorescence Emission Maxima (λex max) of Dyes Dissolved in Four DESs

sample	ANS λex max (nm)	pyrene λex max (nm)	PCHO λex max (nm)	Coumarin12 λex max(nm)	Nile red λex max (nm)
PEG-2/DES-1	468	375	442	459	626
PEG-3//DES-2	464	373	436	443	622
PEG-4/DES-3	467	374	438	456	618
PEG-6/DES-4	458	373	432	436	615

fluorescence responses observed in the spectra, which reflect the interaction between the dye molecules and the solvent environment. The study effectively demonstrates the utility of fluorescence spectroscopy as a method for evaluating solvent polarity, providing essential insights into the characteristics of the synthesized DESs and their potential applications in protein extraction and other biochemical processes.[48,49]

4. EXTRACTION STUDY

4.1. Single-Factor Experiments for Protein Extraction.

4.1.1. Effect of the Volume of DES. Proteins are an amphoteric substance and may be affected by the concentration of DESs in the aqueous phase. The DES-based ATPS is an important factor that affects protein separation. Studies have found that the extraction efficiency of proteins reaches a climax at its isoelectric point. The effectiveness of protein extraction is, therefore, significantly influenced by the electrostatic interaction between the charged group of the protein and the ionic group of DES. Figure 9 displays the volume phase ratio of the top phase and bottom phase developed by different conc. Of DES in ATPS (DES−Na_2CO_3, BHb) and Figure 10 illustrate that efficiency rises significantly when DES content in ATPS increases. The comparative extraction efficiency of BHb using four PEG-based DESs is Shown in (Table S8.). We have taken 1.2, 1.6, 2.0, 2.4 mL of synthesized DESs in 1.6 mL of salt solution (0.6 g/mL) with 20 mg of protein.

4.1.2. Effect of the Concentration of Salt. Another significant element influencing protein separation in DES-based ATPS is the concentration of inorganic ions in the solution. Protein distribution in DES can be enhanced, hydrophobic interaction and protein solubility in water can be decreased by a high concentration of inorganic salts in protein solution, as Figure 11 illustrates, the protein's extraction efficiency starts to decline at high inorganic salt concentrations. When the bottom phase is very hydrophilic, the transfer of the protein into the salt-rich bottom phase is driven by the hydrogen bonding interaction between the

https://doi.org/10.1021/acsomega.4c09125
ACS Omega 2025, 10, 6839−6856

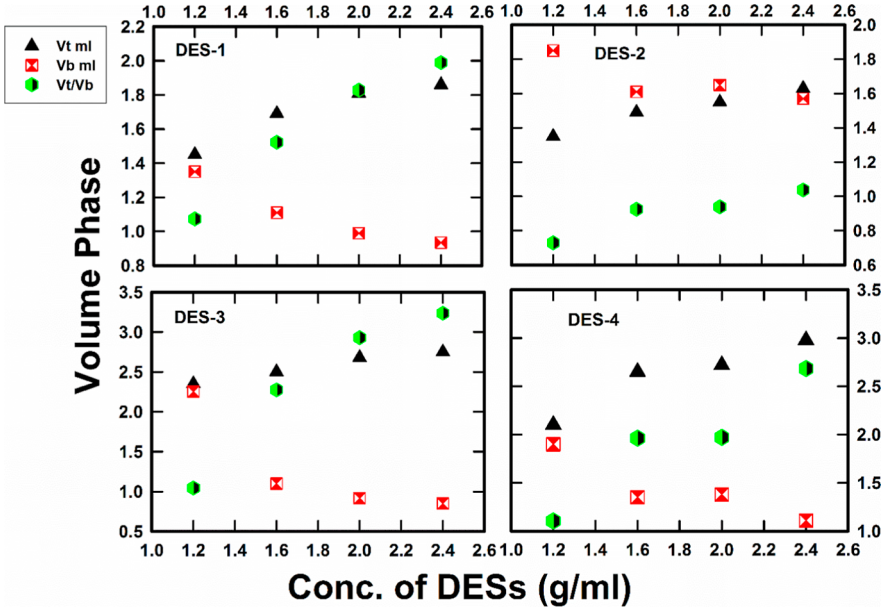

Figure 9. Change in volume phase of ATPS of top phase at different concentrations of DESs (1.2, 1.6, 2.0, and 2.4 mL) with salt conc. 1.6 mL (0.6 g/mL).

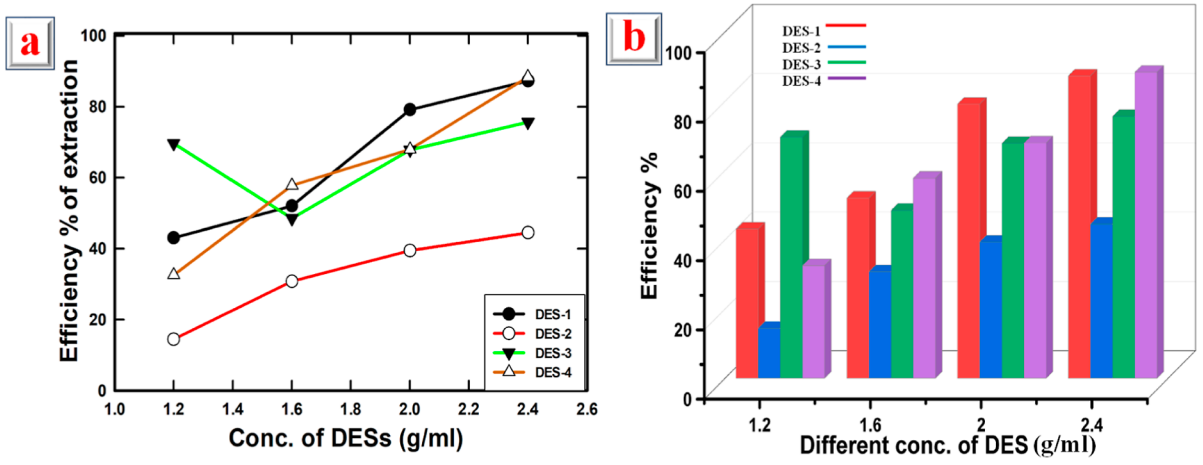

Figure 10. (a) The extraction efficiency in developed ATPS (DES−Na_2CO_3, BHb) at different concentrations of DESs (b) bar graph of (a).

amino acid residues and the water molecules on the protein's surface. Consequently, the primary factor promoting protein transfer into the DES-rich top phase could be hydrophobic interactions, salting out effects, or hydrogen bonding interactions. Figure 12 displays the volume phase ratio of the top and bottom phases developed by different conc. of DES in ATPS (DES−Na_2CO_3, BHb) and Figure 12 illustrates that efficiency decreases significantly when salt conc. in ATPS increase. The comparative extraction efficiency of BHb using four PEG-based DESs is Shown in (Table S9.) We took 2.0 mL of synthesized DESs in 1.6 mL of salt solution (0.6, 0.7, 0.8, 0.9, and 1.0 g/mL) with 20 mg of protein.

4.1.3. Statistical Analysis and Its Implications for Extraction Efficiency. 4.1.3.1. Extraction Efficiency at Different DES Concentrations. The statistical analysis revealed significant differences in the extraction efficiencies of BHb across varying DES concentrations (1.2, 1.6, 2.0, and 2.4 mL). The one-way ANOVA confirmed that DES concentration plays a critical role in protein recovery, with $p < 0.05$ validating the observed trends (Table S10a,b). For DES-3, the extraction efficiency increased steadily with higher DES concentrations, reaching a peak mean efficiency of 75.6% at 2.4 mL. This trend highlights the ability of DES-3 to create a favorable environment for protein partitioning, attributed to its optimal viscosity and hydrogen-bonding interactions. DES-4 similarly achieved high extraction efficiencies, peaking at 88.3% at 2.4 mL, suggesting that higher DES volumes provide better phase separation and protein solubilization. Conversely, DES-2 exhibited lower extraction efficiencies across all concentrations, with a peak efficiency of only 44.5% at 2.4 mL. This lower performance may be due to suboptimal hydrogen bonding and weaker protein−DES interactions, indicating the need for further optimization of DES components for efficient protein recovery. The results confirm that increasing DES concentration generally improves extraction efficiency up to a certain threshold, beyond which saturation effects may occur, as seen with some DESs.

4.1.3.2. Extraction Efficiency at Different Salt Concentrations. The effect of salt concentration on extraction efficiency was equally significant, with ANOVA results

https://doi.org/10.1021/acsomega.4c09125
ACS Omega 2025, 10, 6839−6856

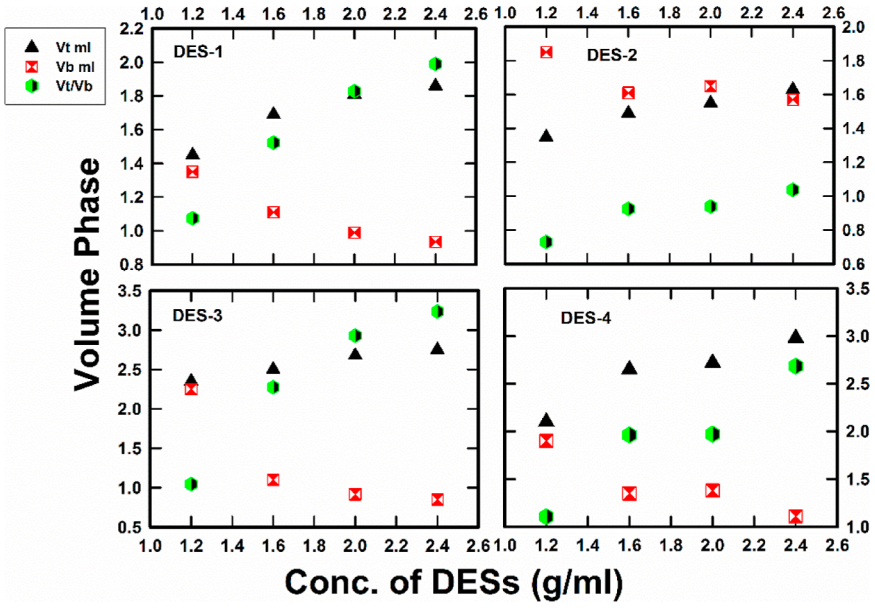

Figure 11. Change in volume phase of ATPS top phase at different concentrations of salt (0.6, 0.7, 0.8, 0.9, and 1.0 g/mL).

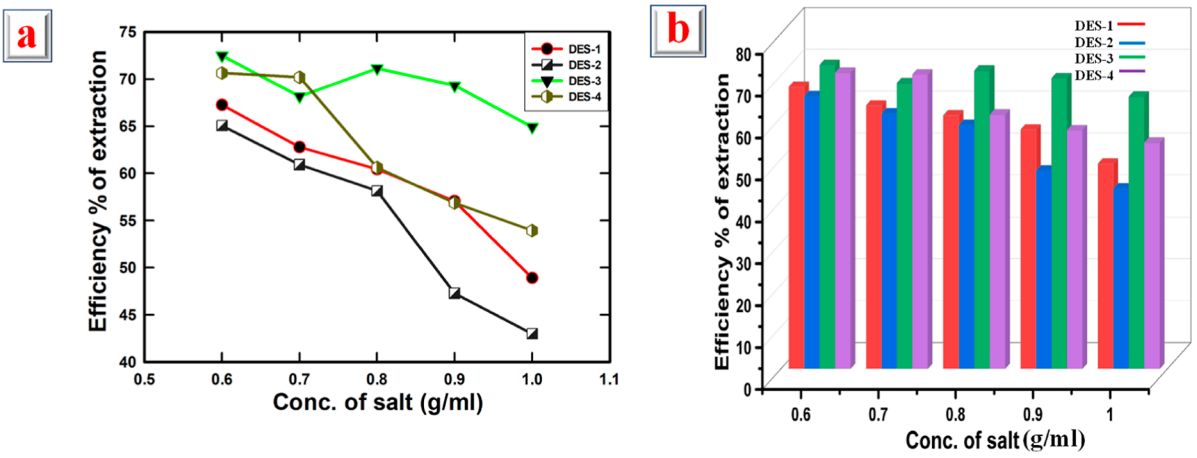

Figure 12. (a) The extraction efficiency in developed ATPS (DES−Na_2CO_3, BHb) at different concentrations of salt (b) Bar graph of (a).

(Table S11a,b). indicating $p < 0.05$. Salt concentration was varied from 0.4 to 1.0 g/mL to evaluate its influence on protein partitioning into the DES-rich phase. DES-3 demonstrated the most consistent performance, achieving a mean extraction efficiency of 72.5% at 1.0 g/mL salt concentration, compared to 64.9% at 0.4 g/mL. This trend aligns with the salting-out effect, where higher ionic strength facilitates protein migration into the DES phase by reducing solubility in the aqueous phase. DES-4 also showed enhanced efficiency, reaching 70.6% at 1.0 g/mL, suggesting its high compatibility with increased ionic strength. In contrast, DES-2 displayed a more variable response, with extraction efficiency ranging from 43.0% at 0.4 g/mL to 65.0% at 1.0 g/mL, indicating that its performance heavily depends on salt concentration. These results emphasize the importance of optimizing salt levels for each DES to maximize extraction efficiency and minimize protein loss.

4.2. Spectroscopic Study of Protein BHb after the Extraction Mechanism with DESs. *4.2.1. UV−Vis Spectroscopy Analysis of Protein−DES Interactions.* Biomacromolecules, such as proteins, are known to act as photoreceptors, meaning they can absorb light at specific wavelengths due to the presence of chromophores, such as aromatic amino acids. In proteins like bovine hemoglobin (BHb), the key chromophores responsible for light absorption include phenylalanine (Phe), tryptophan (Trp), and tyrosine (Tyr) residues. These aromatic residues participate in electronic transitions, which can be monitored by UV−vis spectroscopy to study the structural changes in proteins when exposed to different environmental conditions or interacting molecules such as deep eutectic solvents (DESs). The characteristic absorption peak for pure BHb is typically observed at 614 nm (Figure 13), corresponding to the $n \rightarrow \pi^*$ electronic transition of these aromatic chromophores. This absorption band is crucial for understanding the protein's interaction with DESs, as it reflects changes in the microenvironment of the protein's chromophores during complex formation. The study focuses on how the presence of DESs alters the absorption properties of BHb.

4.2.1.1. Observations and Hypochromic Shift. Figure 13 presents the UV−vis absorption spectra of BHb, demonstrating how its absorption properties change upon interaction with DESs at various concentrations. Following the extraction of BHb with DESs, a noticeable decrease in the absorption peak maximum is observed. Specifically, the absorption maximum

https://doi.org/10.1021/acsomega.4c09125
ACS Omega 2025, 10, 6839−6856

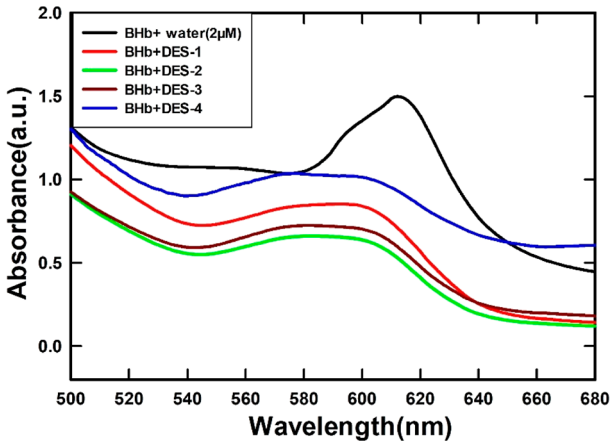

Figure 13. UV−visible absorption spectra of BHb in water and in DES after extraction, illustrating the changes in protein structure and environment upon interaction with DES.

shifts from 614 nm (for pure BHb) to 595 nm for the DES-treated samples. This decrease in absorbance at 595 nm, referred to as a hypochromic shift, is indicative of changes in the local environment around the protein's chromophores. The hypochromic shift observed in the spectra is an important indication that complexation has occurred between the DES molecules and the BHb protein. This shift suggests that the protein is undergoing alterations in its structure, particularly in the arrangement of its aromatic residues, which leads to a change in the absorption characteristics of the protein. The decrease in absorbance indicates that fewer chromophores are excited due to the formation of a ground-state complex between the DES and BHb. This is a classic feature of **static quenching**, where complex formation between the protein and DES reduces the protein's ability to absorb light in the UV−vis range.

4.2.1.2. Implications of Protein−DES Complexation. The observed hypochromic shift and decrease in absorption intensity upon DES extraction imply that the microenvironment surrounding the chromophores in BHb has been altered. This can be attributed to the complexation between the protein and DES molecules, which affects the electronic structure of the chromophores and leads to changes in their light absorption properties. The formation of a ground-state complex between the DES and BHb results in the quenching of the protein's fluorescence and reduction in UV−vis absorbance, which is characteristic of a **static quenching mechanism**.

The UV−vis spectroscopy results provide important insights into the structural changes that occur in BHb when it interacts with DESs. The observed hypochromic shift and reduction in absorbance indicate complexation between the protein and DESs, leading to a change in the microenvironment of the protein's aromatic chromophores. These findings suggest that DESs significantly modulate protein structure and stability, likely through static quenching mechanisms. The observed hypochromic shifts in UV−vis spectra indicate reduced exposure of aromatic residues, suggesting a more compact protein structure. This compaction reflects protein stabilization in the DES-rich phase, minimizing denaturation during extraction. These shifts reflect reduced exposure of aromatic residues, suggesting increased protein compactness or aggregation. The extent of the shift reveals the stabilizing effects of DES through hydrogen bonding, ionic interactions, or hydrophobic effects. Thus, hypochromic shifts are key markers for assessing protein stability and structural modulation in DES environments. The UV−vis results are consistent with the fluorescence spectroscopy data, providing a comprehensive picture of how DESs interact with proteins at the molecular level. Further, spectroscopic studies, such as 3D fluorescence and FT-IR, could shed more light on the precise nature of these interactions and their impact on protein function and stability.

4.2.2. Steady-State Fluorescence Spectra of BHb after the Extraction with DESs. Fluorescence spectroscopy is a valuable tool for studying protein extraction with DESs, offering insights into the molecular interactions and structural changes occurring during the process, after analyzing the spectra as shown in Figure 14, it is observed that there is a shift in the

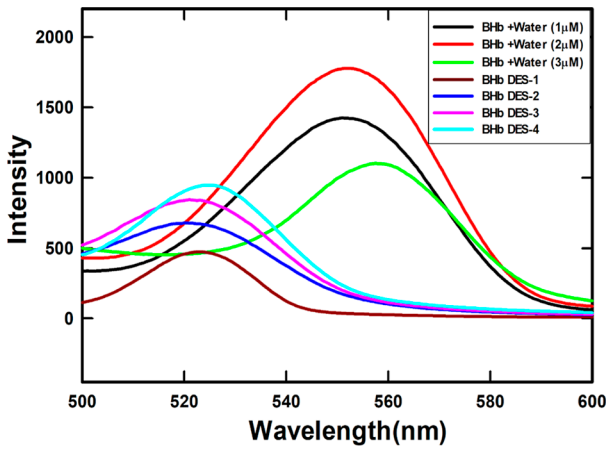

Figure 14. Fluorescence spectra of BHb in water at varying concentrations (1, 2, and 3 μM) compared to its spectra in DESs after extraction, highlighting changes in the protein's microenvironment and interactions with DES.

maximum wavelength of the fluorescence spectra from 550 nm (protein with water) to 520 nm (top phase of ATPS) upon protein extraction with a DES suggests significant alterations in the protein microenvironment. This shift is indicative of changes in the electronic environment around fluorophores within the protein, such as tryptophan and tyrosine residues. One possible explanation is the influence of the DES on the microenvironment, introducing variations in polarity, dielectric constant, or chemical properties compared to water. The observed blue shift suggests a transition to a more hydrophobic environment induced by the DES, potentially leading to changes in protein conformation. Moreover, the shift in fluorescence spectra also signifies conformational changes in the protein structure. The interaction with the DES induces folding or unfolding dynamics, impacting the fluorescence characteristics of the protein. Differential binding affinity between the DES and water could also contribute to the observed shift, indicating that the DES interacts differently with specific regions of the protein containing fluorophores. Additionally, changes in the aggregation state of proteins may be influencing the observed shift. The DES may modulate protein aggregation, leading to shifts in fluorescence spectra. As displayed in Figure 14 the intensity goes on increasing with DES-1 > DES-2 > DES-3 > DES-4 Further experiments and analyses, such as CD spectroscopy and DLS, FT-IR spectroscopy, and 3-D fluoro-spectroscopy, were employed to

https://doi.org/10.1021/acsomega.4c09125
ACS Omega 2025, 10, 6839−6856

Table 3. Distribution of Protein Particles at Different Concentrations of DESs(1.2, 1.6, 2.0, 2.4 mL) with 1.6 mL of Salt Solution (Concentration 0.6 g/mL) in the Top Phase of ATPS

DES sample	parameters	concentration (mL)			
		1.2	1.6	2.0	2.4
DES-1	size (d, nm)	9876	8350	7761	2869
	PDI	0.788	0.700	0.458	0.545
DES-2	size (d, nm)	5317	5175	5813	6939
	PDI	0.722	0.660	0.047	0.907
DES-3	size (d, nm)	10,200	9444	6384	7415
	PDI	0.678	0.636	0.394	1.0
DES-4	size (d, nm)	30,500	28,690	27,160	25,000
	PDI	1.0	1.0	1.0	1.0

investigate changes in protein structure, aggregation, and overall stability during the protein extraction process with DESs and support the above result.

4.3. Distribution of Protein Particle. A method for figuring out the size distribution profile of tiny particles of protein in water and after the extraction of DES solution is DLS spectroscopy. By examining the temporal variations in the intensity of scattered light, it quantifies the thermal random movement (Brownian Motion) of the particles. The hydrodynamic measurements were carried out in a quartz cuvette of 1 cm path length by considering the viscosity and refractive indices of the solutions prepared. The data evaluation of the DLS measurements was performed with the inbuilt CONTIN algorithm. The error observed in the size of the native vesicles and lipoplexes was +8 nm. To sufficiently comprehend the extraction mechanism, the microstructure of the bottom phase was observed by DLS. In this study, proteins were suspended in an ATPS, where the top phase consisted of varying concentrations of DES, while the bottom phase contained a constant concentration of salt. The measurements reflect how DES concentrations influence the microstructure of protein particles, particularly their size and polydispersity index (PDI). PDI is an indicator of the distribution of particle sizes. A lower PDI suggests a more uniform size distribution, while a higher PDI indicates a broader distribution.[28] As mentioned in Table 3 particle size varies with the concentration of DES. Generally, an increase in DES concentration tends to decrease particle size. DES-2 at 2.0 mL has a significantly lower PDI, suggesting a more homogeneous particle size distribution. DES-3 at 2.4 mL has a high PDI, indicating a broad range of particle sizes. These observations provide insights into how different concentrations of DESs in the ATPS impact the size distribution of protein particles.

4.3.1. Size Distribution and PDI. 4.3.1.1. DES-1. At 1.2 mL concentration, DES-1 shows a very large particle size of 9876 nm, indicating significant aggregation or particle clustering. However, with increasing DES concentration (2.0 and 2.4 mL), a notable reduction in particle size is observed (7761 to 2869 nm). This decrease suggests that the DES may have a dispersive effect on the protein particles. The PDI also shifts from 0.788 to 0.545, indicating that the system becomes more homogeneously distributed with increasing concentration, though there's still moderate polydispersity at higher concentrations.

4.3.1.2. DES-2. This sample exhibits a relatively consistent particle size across different concentrations (5317 to 6939 nm). However, the PDI values indicate significant changes in particle homogeneity. At 2.0 mL, DES-2 exhibits a very low PDI of 0.047, suggesting an exceptionally narrow size distribution. Conversely, at 2.4 mL, the PDI increases sharply to 0.907, suggesting a more heterogeneous system. This suggests that DES-2 achieves optimal dispersion and homogeneity at 2.0 mL concentration, beyond which aggregation might begin to occur.

4.3.1.3. DES-3. The size distribution for DES-3 fluctuates significantly. At 1.6 mL, a high size of 9444 nm is observed, followed by a reduction at 2.0 mL (6384 nm) and a subsequent increase at 2.4 mL (7415 nm). The PDI values, ranging from 0.678 to 1.0, indicate moderate to significant polydispersity, with the system becoming highly heterogeneous at 2.4 mL. This suggests that DES-3 may cause aggregation at higher concentrations, possibly due to oversaturation or poor solvent−particle interactions at these concentrations.

4.3.1.4. DES-4. Across all concentrations, DES-4 shows very high particle sizes (28,690 to 27,160 nm) and a consistently high PDI of 1.0, indicating a highly polydisperse and likely unstable system. The large size suggests that this DES causes excessive aggregation or clustering, which could be due to either poor solubility or incompatibility with the proteins in this system. The lack of meaningful reduction in size across concentrations reinforces that DES-4 may not be an effective solvent for this type of application.

4.3.2. Effect of DES Concentration on Particle Size. The data shows that the concentration of DES plays a crucial role in determining the size and distribution of protein particles in the ATPS system.

In general, a lower concentration of DES tends to result in larger particle sizes, possibly due to poor solvation or incomplete interaction between the protein and DES. As the concentration of DES increases (particularly for DES-1 and DES-2), particle sizes tend to decrease, suggesting that higher DES concentrations provide better solvation and stabilization of the proteins, preventing aggregation. However, beyond certain thresholds (e.g., 2.4 mL for DES-3 and DES-4), the particle size increases again, potentially indicating aggregation due to excessive DES saturation or destabilization of the system.

4.3.3. PDI Insights. PDI, or polydispersity index, is a measure of the uniformity of particle size distribution. A lower PDI (closer to 0) indicates a more uniform distribution, while higher PDI values suggest greater size heterogeneity.

DES-2 at 2.0 mL shows the lowest PDI (0.047), suggesting a highly uniform particle size distribution at this concentration, which is desirable in applications requiring homogeneous particle behavior. In contrast, DES-4 shows a consistently high PDI of 1.0 across all concentrations, indicating a broad range of particle sizes, likely due to aggregation or destabilization of the protein particles in the ATPS system.

https://doi.org/10.1021/acsomega.4c09125
ACS Omega 2025, 10, 6839−6856

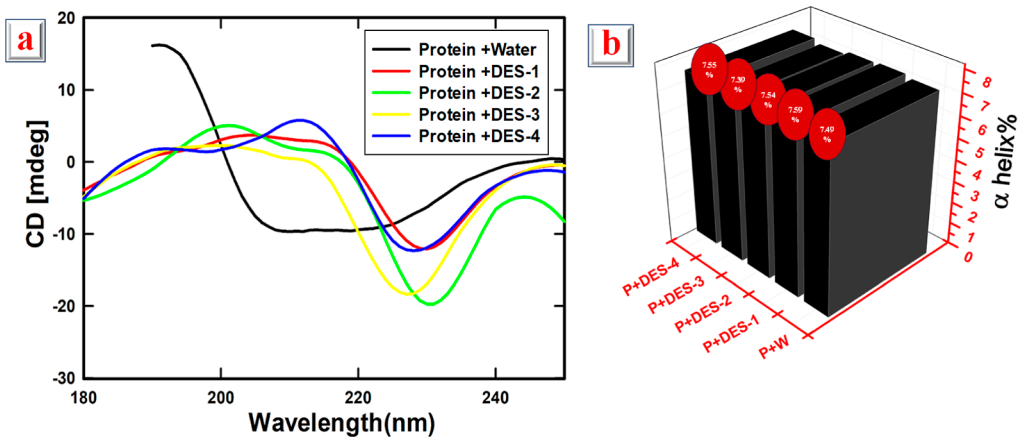

Figure 15. (a) Far-UVCD spectra of BHb with water and with DESs after the extraction (b) bar diagram of α-helix content ([BHb] = 3 μM, T = 298 K, pH = 7.4).

4.3.4. Implications for Protein Extraction. The differences in particle size and PDI with varying DES concentrations reveal key insights into the behavior of proteins in ATPS. DES-2 appears to be the most effective in creating a homogeneous and stable system at 2.0 mL, while DES-4 is ineffective across all concentrations tested. DES-1 shows promise at higher concentrations (2.0 and 2.4 mL) as it significantly reduces particle size while maintaining moderate homogeneity. The performance of DES-3 is variable, with a potential for improved results at intermediate concentrations. This study demonstrates that different DES concentrations can significantly influence the size and distribution of protein particles in an ATPS system. DES-2 at 2.0 mL provides the most uniform particle distribution, while DES-1 is effective at reducing particle size at higher concentrations. DES-4 is ineffective, as indicated by consistently high particle sizes and PDI values. These findings are critical for optimizing protein extraction protocols using DESs, providing insights into the concentration-dependent behavior of DESs in aqueous systems.

4.4. Confirmation of Protein Structure in DES Rich Top Phase and Conformational Changes. In this study, CD spectroscopy was used to analyze the effects of different DESs on the secondary structure of a model protein. Specifically, the focus was on changes in the α-helix content, as DESs are known to influence protein structure due to their unique solvent properties. Protein secondary structure can be identified using CD spectra in the Far-UV range (185−250 nm), where the chromophore is the peptidic bond. Each of the three structures—α helix, beta-sheet, and random coil—produces a distinct CD spectrum with a distinct shape and size. CD spectroscopy is an absorption-based approach that reveals the protein's secondary and tertiary structures. Different kinds of regular secondary structures in proteins produce distinctive CD spectra in the far-UV portion of the spectrum (190−240 nm).[50] The α-helix, β-sheet, β-turn, and other components of the CD spectrum in this region can be examined. Peptide bonds absorb the polarized light in this far UV region. CD signals are generated mainly by the aromatic residues (Phe, Tyr, and Trp).[30,51] Figure 15 displays the samples' CD spectra. The parent protein's maximum peak when dissolved in water (2 μM) was observed in the region of 210−225 nm.

4.4.1. CD Spectroscopy of Protein Secondary Structure. Proteins exhibit distinct CD spectra in the far-UV range (185−250 nm) due to the absorption of polarized light by the peptide bonds, which act as chromophores. The characteristic CD signals of proteins provide information on their secondary structure, including α-helix, β-sheet, and random coil elements. Each structural motif produces a specific pattern in the CD spectrum:

α-helix: Typically shows double minima at 208 and 222 nm.
β-sheet: Exhibits a negative peak near 217 nm.
Random coil: Presents a minimum near 200 nm.

The parent protein (P) in an aqueous solution displayed a characteristic CD signal with a maximum peak observed between 210 and 225 nm. This indicated that the protein maintained its typical secondary structure when dissolved in water.

4.4.2. Effect of DESs on Protein Structure. After extraction with different DESs, the CD spectra exhibited noticeable shifts in the peak positions. The measured peaks for proteins extracted with DES-1, DES-2, DES-3, and DES-4 were found at 232, 230, 229, and 230 nm, respectively. These shifts suggest that the interactions with DESs caused structural alterations to the protein. While the magnitude of the shifts was not drastic, it is clear that the protein underwent conformational changes. The extraction process with DESs seems to have affected the protein's secondary structure, likely by altering the hydrogen bonding and electrostatic interactions that stabilize the α-helix. The most prominent shifts were observed for DES-3, indicating a stronger influence of this particular solvent on the protein structure.

4.4.3. Quantification of α-Helix Content. To quantify the changes in protein structure, the mean residue ellipticity (MRE) values at 222 nm were used to calculate the percentage of α-helix content. The following formulas (eqs S1 and S2) were employed for the calculations (detailed in Supporting Information): the α-helix percentages for the protein (P) and its complexes with DESs (P + DES-1, P + DES-2, P + DES-3, and P + DES-4) were calculated and are presented in the Table S10: The data indicates that the α-helix content of the protein is slightly altered after extraction with different DESs. While the changes in α-helix percentage are not drastic, they do reflect the subtle but significant impact of DESs on the protein's secondary structure. Notably, DES-3 caused the largest reduction in α-helix content, which aligns with the observed shift in the CD spectrum. The shifts in the CD spectra and changes in α-helix content suggest that the interaction between the protein and DESs leads to a partial

https://doi.org/10.1021/acsomega.4c09125
ACS Omega 2025, 10, 6839−6856

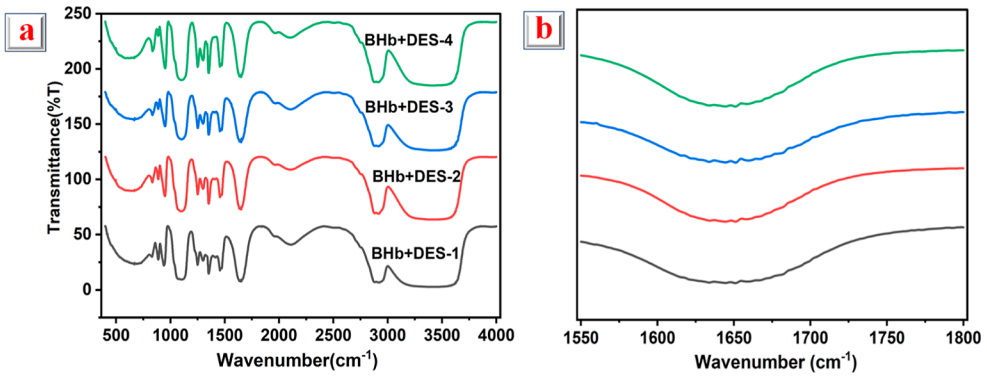

Figure 16. (a) FT-IR spectra of BHb with four synthesized DESs after the extraction (b) amide I, amide II, and amide III bands region spectra of (a).

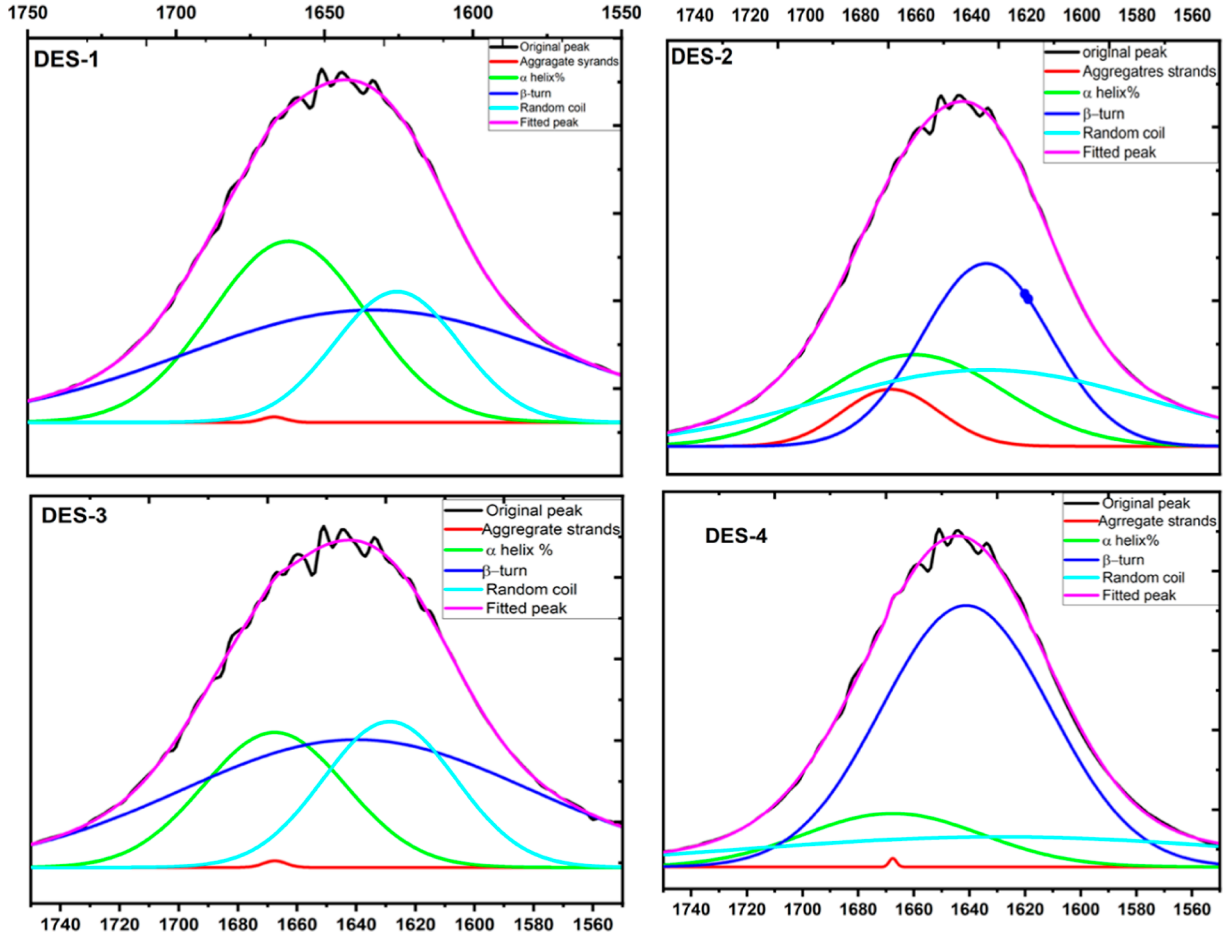

Figure 17. Deconvolution of the amide I and amide II bands in the FT-IR spectra of BHb with four synthesized DESs after the extraction.

unfolding or rearrangement of the secondary structure. This is consistent with previous studies that have shown that DESs can disrupt the native structure of proteins by altering the hydration shell and weakening intramolecular interactions. Among the four DESs tested, DES-3 had the most pronounced effect on the protein structure, as evidenced by both the peak shifts in the CD spectrum and the reduction in α-helix content. This may be attributed to the specific chemical composition and molecular interactions of DES-3 with the protein. Further studies, such as FT-IR spectroscopy and 3-D fluorescence spectroscopy, could provide additional insights into the specific molecular interactions between DESs and proteins. These techniques would help elucidate whether the observed structural changes are due to the breaking of hydrogen bonds, changes in hydrophobic interactions, or other factors.[28]

4.4.4. FT-IR Spectroscopy. FT-IR spectroscopy is an important tool to study the structural transition in biomolecules like protein etc. Here, FT-IR spectroscopy was employed to investigate the conformational changes in BHb. The infrared spectrum (IR) characteristic peaks of amide I and amide II bands are marked as amide or peptide characteristic peaks, obtained in the region 1550−1800 cm^{-1} due to the change of secondary structure of BHb Figure 16. The deconvolution of this band has been done to analyze the

https://doi.org/10.1021/acsomega.4c09125
ACS Omega 2025, 10, 6839−6856

protein secondary structure, which is shown in Figure 17. With the help of the deconvolution plot, we calculate the α helix %, β-turn, random coil, aggregate strands has been calculated which are given in Table 4.

Table 4. Conformation Analysis of Protein DESs ATPS (Top Phase) Using FT-IR Analysis Which is Determined from the Deconvolution of the Amide Bands Region in the FT-IR Spectra

samples	α-helix [%]	β-sheet [%]	random coil [%]	others [%]
PEG-2/DES-1	32.36	48.66	18.82	0.15
PEG-3//DES-2	23.19	33.30	35.66	7.8
PEG-4/DES-3	24.08	53.53	23.20	0.18
PEG-6/DES-4	13.86	64.11	21.92	0.090

4.4.5. Three-Dimensional Fluorescence Spectra of BHb after the Extraction with DESs. The 3D fluorescence spectra in Figure 18 provide critical insights into the structural changes of bovine hemoglobin (BHb) upon interaction with various synthesized DESs. The spectra were recorded for the following samples:

- Pure BHb protein in water
- BHb protein extracted with DES-1
- BHb protein extracted with DES-2
- BHb protein extracted with DES-3
- BHb protein extracted with DES-4

In the spectrum of pure BHb protein in water (spectrum a), three distinct peaks are observed, which are indicative of the intrinsic fluorescence properties of the protein. These peaks typically correspond to the emission wavelengths associated with the tryptophan residues, which are sensitive to their local environment.[52] The peaks can be summarized as follows:

- **Peak 1**: Located around 330 nm, this peak is primarily due to the emission from tryptophan residues, reflecting the native conformation of the protein.
- **Peak 2**: Found at approximately 350 nm, this peak may indicate interactions between tryptophan and nearby aromatic residues or changes in the microenvironment that affect the emission characteristics.
- **Peak 3**: Observed around 450 nm, this peak could be associated with the presence of heme groups or other chromophores within the protein, contributing to the overall fluorescence profile.

In comparing the spectra from (b) to (e), significant changes in the emission characteristics of BHb are noted upon extraction with the various DESs.

- (b) **(BHb + DES-1):** The peaks show a slight red shift, with Peak 1 moving to around 335 nm. The fluorescence intensity decreases, suggesting moderate structural changes and a more polar environment around the tryptophan residues, indicating that DES-2 has a mild effect on the protein structure.
- (c) **(BHb + DES-2):** The emission peaks are further red-shifted, with Peak 1 observed at approximately 340 nm and a notable reduction in intensity. This indicates more substantial structural alterations, potentially leading to a more exposed conformation of the protein. The changes suggest that DES-3 interacts more strongly with the protein, affecting its fluorescence properties.
- (d) **(BHb + DES-2):** Similar to DES-2, the peaks show a redshift, with Peak 1 around 342 nm. The intensity continues to decrease, indicating that DES-4 induces significant structural changes, possibly affecting the protein's tertiary structure.
- (e) **(BHb + DES-4):** This spectrum exhibits the most pronounced changes, with Peak 1 shifting to approximately 345 nm and a dramatic reduction in fluorescence intensity. This suggests that DES-6 induces extensive structural alterations, potentially leading to denaturation or unfolding of the protein, as indicated by the extensive quenching of the tryptophan residues.

The analysis of the 3D fluorescence spectra reveals that the interaction between BHb and the DESs leads to varying degrees of structural changes, depending on the specific DES composition. The distinct peaks observed in the pure protein spectrum serve as a baseline for assessing the impact of the DESs on protein structure and stability. The findings highlight the effectiveness of fluorescence spectroscopy in elucidating the structural dynamics of proteins during extraction processes. These insights are crucial for maintaining protein functionality and ensuring the quality of extracted protein products, further supporting the potential application of DESs in biotechnological processes.[52−54]

5. CONCLUSION

In this study, we successfully prepared DESs composed of BTEAC and PEG at varying molecular weights (200, 300, 400, and 600) to explore their potential for protein extraction. The prepared DESs were comprehensively characterized using FT-IR, NMR, viscosity, density, and polarity assessments. The findings indicated that these DESs exhibit favorable physicochemical properties, making them suitable candidates for protein extraction applications.[55−58] Among the DESs studied, DES-4 (PEG-600) was identified as the most suitable for protein extraction due to its optimal viscosity and polarity, which facilitated efficient phase separation and minimal protein conformational changes.[59] These properties make DES-4 a promising candidate for sustainable and scalable protein extraction. This study explores PEG-based DESs as environmentally friendly solvents for protein extraction, with potential applications in the biotechnology and pharmaceutical industries. DES-4 achieved the highest extraction efficiency of 88% while preserving protein structure, emphasizing its potential for industrial applications. The extraction studies revealed significant changes in the molecular structure of the target protein, bovine hemoglobin (BHb), as evidenced by UV spectroscopy, 3D fluorescence, DLS, and CD analyses. Ionic interactions between the chloride ions in BTEAC and charged regions of BHb stabilize the DES-protein complex. These interactions, combined with hydrogen bonding, facilitate selective extraction by reducing protein aggregation and enhancing solubility in the DES phase.[60] The formation of a biphasic system during the extraction process further demonstrated the effectiveness of DESs in selectively isolating proteins while preserving their structural integrity. While the DES quantity may appear significant, conventional solvents such as ethanol or methanol require similar or greater volumes for comparable protein recovery. The comparative analysis highlights that the extraction efficiency of PEG-based DESs in this study exceeds that of choline chloride-based DESs reported in previous studies.[61] This improvement is likely

https://doi.org/10.1021/acsomega.4c09125
ACS Omega 2025, 10, 6839−6856

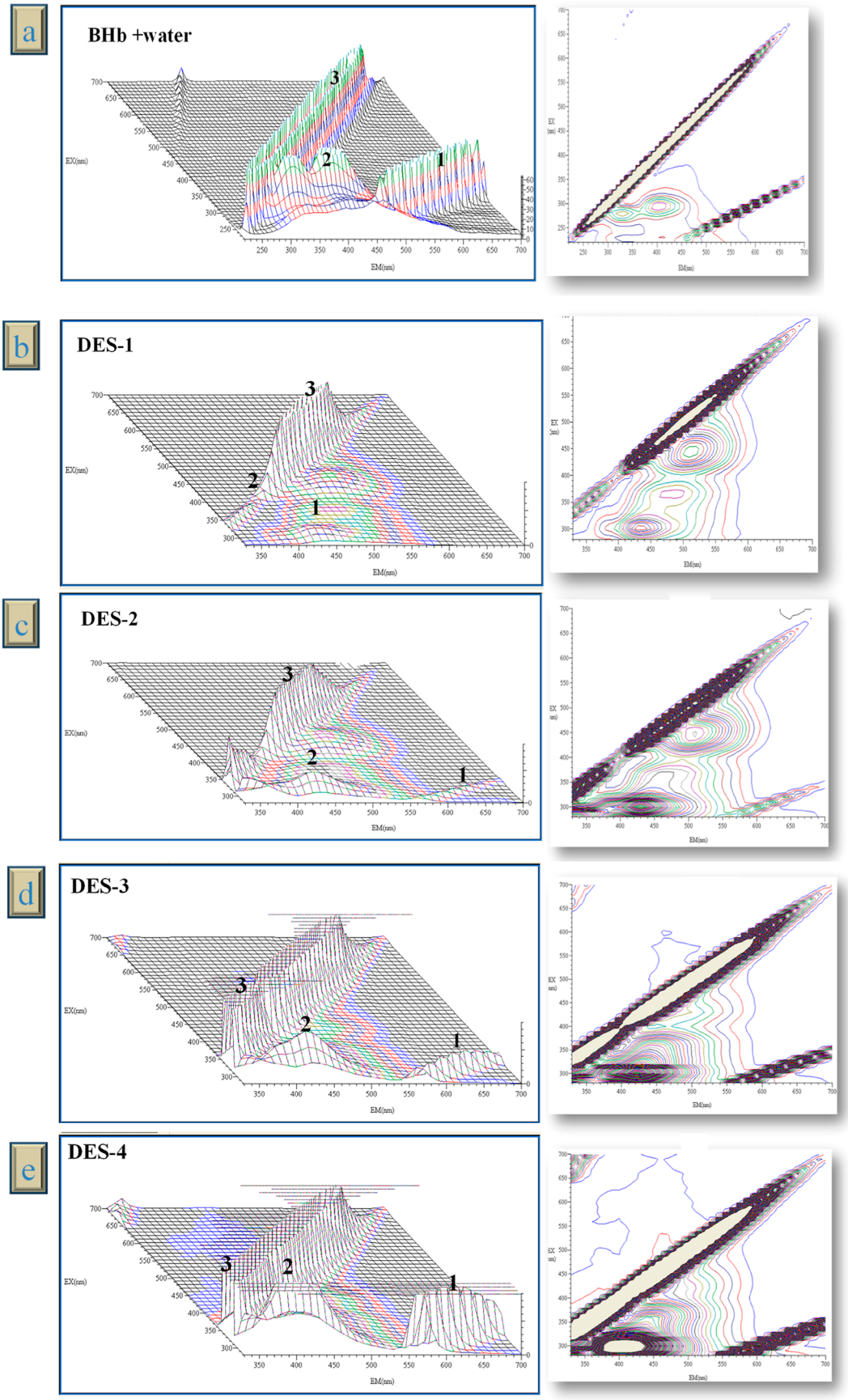

Figure 18. 3-D fluorescence spectra with contour plot (a) BHb + water and following DESs after the extraction (b) BHb + DES-1, (c) BHb + DES-2, (d) BHb + DES-3 and (e) BHb + DES-4.

https://doi.org/10.1021/acsomega.4c09125
ACS Omega 2025, 10, 6839−6856

due to PEG's superior hydrogen bonding capacity and compatibility with proteins, highlighting its potential for broader applications. Looking ahead, the successful application of DESs in protein extraction opens up new avenues for their use in biotechnological processes, including the extraction of bioactive compounds and other biomolecules. The scalability of PEG-based DESs is promising, given their reusability and the moderate cost of PEG components. Additionally, preliminary cytotoxicity tests confirm their biocompatibility, making them suitable for applications in protein therapeutics and drug delivery.[62−64] The stronger protein−DES interactions observed with DES-4 (PEG-600) can be attributed to its higher molecular weight, which enhances hydrophobic and hydrogen bonding interactions. These interactions stabilize the protein structure, making DES-4 particularly effective in preserving protein integrity during extraction. Further studies explore cost-effective production methods for large-scale implementation. Although PEG-based DESs are biocompatible and effective, their high viscosity may pose challenges for large-scale mixing and phase separation.[65−67] Future studies should focus on optimizing DESs compositions to reduce viscosity without compromising extraction efficiency. Overall, this study highlights the potential of DESs as versatile tools in the field of protein extraction and purification and provides a foundation for sustainable green bioprocesses.[16,68−70]

■ ASSOCIATED CONTENT

Supporting Information

The Supporting Information is available free of charge at https://pubs.acs.org/doi/10.1021/acsomega.4c09125.

Structures of prepared PEG-based DESs (Figure S1), density variation with temperature and fitted curve (Figure S2, Table S1), dynamic viscosity variation and Arrhenius fitting parameters (Figure S3, Tables S2−S4), kinematic viscosity variation and VFT fitting parameters (Figure S4, Tables S5−S7), extraction efficiencies of BHb with DESs at varying concentrations and salt levels (Tables S8 and S9), statistical analysis of extraction efficiencies (Tables S10 and S11) and α-helical content of proteins in DESs and water (Table S12) (PDF)

■ AUTHOR INFORMATION

Corresponding Author

Maroof Ali − *Department of Chemistry, Aligarh Muslim University, Aligarh, Uttar Pradesh 202002, India;* orcid.org/0000-0003-0296-5327; Email: mdmaroof@gmail.com, maroof.ch@amu.ac.in

Authors

Masooma Siddiqui − *Department of Chemistry, Aligarh Muslim University, Aligarh, Uttar Pradesh 202002, India*

Md Sayem Alam − *Council of Scientific and Industrial Research (CSIR)−Central Leather Research Institute (CLRI), Polymer Science & Technology, Chennai 600 020, India;* orcid.org/0000-0001-9944-1620

Complete contact information is available at: https://pubs.acs.org/10.1021/acsomega.4c09125

Notes

The authors declare no competing financial interest.

■ ACKNOWLEDGMENTS

I would like to acknowledge the Department of Chemistry AMU for providing a conducive environment for this research. And thanks, UGC for Non -NET fellowship.

■ REFERENCES

(1) Ma, Y.; Yang, Y.; Li, T.; Hussain, S.; Zhu, M. Deep Eutectic Solvents as an Emerging Green Platform for the Synthesis of Functional Materials. *Green Chem.* **2024**, *26* (7), 3627−3669.

(2) Vieira Sanches, M.; Freitas, R.; Oliva, M.; Mero, A.; De Marchi, L.; Cuccaro, A.; Fumagalli, G.; Mezzetta, A.; Colombo Dugoni, G.; Ferro, M.; Mele, A.; Guazzelli, L.; Pretti, C. Are Natural Deep Eutectic Solvents Always a Sustainable Option? A Bioassay-Based Study. *Environ. Sci. Pollut. Res.* **2023**, *30* (7), 17268−17279.

(3) Herce-Sesa, B.; López-López, J. A.; Moreno, C. Advances in Ionic Liquids and Deep Eutectic Solvents-Based Liquid Phase Microextraction of Metals for Sample Preparation in Environmental Analytical Chemistry. *TrAC, Trends Anal. Chem.* **2021**, *143*, 116398.

(4) Taghizadeh, M.; Taghizadeh, A.; Vatanpour, V.; Ganjali, M. R.; Saeb, M. R. Deep Eutectic Solvents in Membrane Science and Technology: Fundamental, Preparation, Application, and Future Perspective. *Sep. Purif. Technol.* **2021**, *258*, 118015.

(5) Plastiras, O.-E.; Samanidou, V. Applications of Deep Eutectic Solvents in Sample Preparation and Extraction of Organic Molecules. *Molecules* **2022**, *27* (22), 7699.

(6) de Andrade, D. C.; Monteiro, S. A.; Merib, J. A Review on Recent Applications of Deep Eutectic Solvents in Microextraction Techniques for the Analysis of Biological Matrices. *Adv. Sample Prep.* **2022**, *1*, 100007.

(7) Fernández, M. d. l. Á.; Boiteux, J.; Espino, M.; Gomez, F. J. V.; Silva, M. F. Natural Deep Eutectic Solvents-Mediated Extractions: The Way Forward for Sustainable Analytical Developments. *Anal. Chim. Acta* **2018**, *1038*, 1−10.

(8) Dwamena, A. K. Recent Advances in Hydrophobic Deep Eutectic Solvents for Extraction. *Separations* **2019**, *6*, 9.

(9) Li, X.; Row, K. H. Development of Deep Eutectic Solvents Applied in Extraction and Separation. *J. Sep. Sci.* **2016**, *39* (18), 3505−3520.

(10) Zeng, Q.; Wang, Y.; Huang, Y.; Ding, X.; Chen, J.; Xu, K. Deep Eutectic Solvents as Novel Extraction Media for Protein Partitioning. *Analyst* **2014**, *139* (10), 2565−2573.

(11) Pena-Pereira, F.; Namieśnik, J. Ionic Liquids and Deep Eutectic Mixtures: Sustainable Solvents for Extraction Processes. *ChemSusChem* **2014**, *7* (7), 1784−1800.

(12) Huang, J.; Guo, X.; Xu, T.; Fan, L.; Zhou, X.; Wu, S. Ionic Deep Eutectic Solvents for the Extraction and Separation of Natural Products. *J. Chromatogr. A* **2019**, *1598*, 1−19.

(13) Dardavila, M. M.; Pappou, S.; Savvidou, M. G.; Louli, V.; Katapodis, P.; Stamatis, H.; Magoulas, K.; Voutsas, E. Extraction of Bioactive Compounds from C. Vulgaris Biomass Using Deep Eutectic Solvents. *Molecules* **2023**, *28* (1), 415.

(14) Grudniewska, A.; M. de Melo, E.; Chan, A.; Gniłka, R.; Boratyński, F.; S Matharu, A. Enhanced Protein Extraction from Oilseed Cakes Using Glycer Deep Eutectic Solvents: A Biorefinery Approach. *ACS Sustainable Chem. Eng.* **2018**, *6* (11), 15791−15800.

(15) Zhang, H.; Wang, Y.; Xu, K.; Li, N.; Wen, Q.; Yang, Q.; Zhou, Y. Ternary and Binary Deep Eutectic Solvents as a Novel Extraction Medium for Protein Partitioning. *Anal. Methods* **2016**, *8* (46), 8196−8207.

(16) Vladić, J.; Jakovljević Kovač, M.; Pavić, V.; Jokić, S.; Simić, S.; Paiva, A.; Jerković, I.; Duarte, A. R. Towards a Greener Approach for Biomass Valorization: Integration of Supercritical Fluid and Deep Eutectic Solvents. *Antibiotics* **2023**, *12* (6), 1031.

(17) Perna, F. M.; Vitale, P.; Capriati, V. Deep Eutectic Solvents and Their Applications as Green Solvents. *Curr. Opin. Green Sustainable Chem.* **2020**, *21*, 27−33.

(18) Dai, Y.; van Spronsen, J.; Witkamp, G. J.; Verpoorte, R.; Choi, Y. H. Natural Deep Eutectic Solvents as New Potential Media for Green Technology. *Anal. Chim. Acta* **2013**, *766*, 61−68.
(19) Nam, N. N.; Do, H. D. K.; Trinh, K. T. L.; Lee, N. Y. Design Strategy and Application of Deep Eutectic Solvents for Green Synthesis of Nanomaterials. *Nanomaterials* **2023**, *13*, 1164.
(20) Ling, J. K. U.; Hadinoto, K. Deep Eutectic Solvent as Green Solvent in Extraction of Biological Macromolecules: A Review. *Int. J. Mol. Sci.* **2022**, *23*, 3381.
(21) Krishnan, A.; Gopinath, K. P.; Vo, D. V. N.; Malolan, R.; Nagarajan, V. M.; Arun, J. Ionic Liquids, Deep Eutectic Solvents and Liquid Polymers as Green Solvents in Carbon Capture Technologies: A Review. *Environ. Chem. Lett.* **2020**, *18*, 2031−2054.
(22) Chen, Y.; Li, G.; Yu, S.; Guo, Z.; Dong, Z.; Wang, S. Efficient Iodine Capture by Biocompatible PEG-Based Deep Eutectic Solvents: Kinetics and Dynamic Mechanism. *J. Mol. Liq.* **2019**, *289*, 111166.
(23) Chen, W.; Bai, X.; Xue, Z.; Mou, H.; Chen, J.; Liu, Z.; Mu, T. The Formation and Physicochemical Properties of PEGylated Deep Eutectic Solvents. *New J. Chem.* **2019**, *43* (22), 8804−8810.
(24) Xue, Z.; Xue, Z. The High-Efficiency and Eco-Friendly PEGylated Ionic Liquid Systems for Radioactive Iodine Capture through Halogen Bonding Interaction. *J. Mol. Liq.* **2017**, *238*, 106−114.
(25) Meng, J.; Wang, Y.; Zhou, Y.; Chen, J.; Wei, X.; Ni, R.; Liu, Z.; Xu, F. Development of Different Deep Eutectic Solvent Aqueous Biphasic Systems for the Separation of Proteins. *RSC Adv.* **2019**, *9* (25), 14116−14125.
(26) Marchel, M.; Coroadinha, A. S.; Marrucho, I. M. Novel Acidic Deep Eutectic Solvent-Based Aqueous Biphasic Systems for Efficient Extraction of Pepsin. *ACS Sustain. Chem. Eng.* **2020**, *8* (33), 12400−12408.
(27) Xu, K.; Xu, P.; Wang, Y. Aqueous Biphasic Systems Formed by Hydrophilic and Hydrophobic Deep Eutectic Solvents for the Partitioning of Dyes. *Talanta* **2020**, *213*, 120839.
(28) Bhakuni, K.; Yadav, N.; Venkatesu, P. A Novel Amalgamation of Deep Eutectic Solvents and Crowders as Biocompatible Solvent Media for Enhanced Structural and Thermal Stability of Bovine Serum Albumin. *Phys. Chem. Chem. Phys.* **2020**, *22* (42), 24410−24422.
(29) Kumari, M.; Kumari, P.; Kashyap, H. K. Structural Adaptations in the Bovine Serum Albumin Protein in Archetypal Deep Eutectic Solvent Reline and Its Aqueous Mixtures. *Phys. Chem. Chem. Phys.* **2022**, *24* (9), 5627−5637.
(30) Miles, A. J.; Drew, E. D.; Wallace, B. A. DichroIDP: A Method for Analyses of Intrinsically Disordered Proteins Using Circular Dichroism Spectroscopy. *Commun. Biol.* **2023**, *6* (1), 823.
(31) Lopes, J. L. S.; Miles, A. J.; Whitmore, L.; Wallace, B. A. Distinct Circular Dichroism Spectroscopic Signatures of Polyproline II and Unordered Secondary Structures: Applications in Secondary Structure Analyses. *Protein Sci.* **2014**, *23* (12), 1765−1772.
(32) Hu, Y.; Liang, P.; Wang, Z.; Zhu, H.; Liu, Q. Developing Amino Acid-Citric Acid-Based Deep Eutectic Solvent for Food Applications: Preparation, Characterization, Antibacterial Activity, Biosafety, and Formation Mechanism Exploration. *Sustainable Chem. Pharm.* **2023**, *36*, 101317.
(33) Liu, X.; Zhai, Y.; Xu, Z.; Zhu, Y.; Zhou, Y.; Wang, Z.; Liu, L.; Ren, W.; Xie, Y.; Li, C.; Xu, M. The Novel Application of Type II Deep Eutectic Solvents (DES) for Sludge Dewatering. *Sep. Purif. Technol.* **2023**, *306*, 122714.
(34) Suthar, P.; Kaushal, M.; Vaidya, D.; Thakur, M.; Chauhan, P.; Angmo, D.; Kashyap, S.; Negi, N. Deep Eutectic Solvents (DES): An Update on the Applications in Food Sectors. *J. Agric. Food Res.* **2023**, *14*, 100678.
(35) Zhang, M.; Zhang, Z.; Gul, Z.; Tian, M.; Wang, J.; Zheng, K.; Zhao, C.; Li, C. Advances of Responsive Deep Eutectic Solvents and Application in Extraction and Separation of Bioactive Compounds. *J. Sep. Sci.* **2023**, *46*, 2300098.
(36) Hayyan, M. Versatile Applications of Deep Eutectic Solvents in Drug Discovery and Drug Delivery Systems: Perspectives and Opportunities. *Asian J. Pharm. Sci.* **2023**, *18*, 100780.
(37) Kamal El-Deen, A.; Abdallah, N.; Elmansi, H.; Belal, F.; Magdy, G. Applications of Deep Eutectic Solvents in Microextraction and Chromatographic Separation Techniques: Latest Developments, Challenges, and Prospects. *Talanta* **2023**, *265*, 124813.
(38) Siddiqui, M.; Alam, M. S.; Ali, M. Preparation and Characterization of Novel Polyols-Based DESs and Their Use in Efficient Sequestration of Radioactive Iodine. *J. Mol. Liq.* **2024**, *412*, 125883.
(39) Zhou, Y.; Wu, W.; Zhang, N.; Soladoye, O. P.; Zhang, Y.; Fu, Y. Deep Eutectic Solvents as New Media for Green Extraction of Food Proteins: Opportunity and Challenges. *Food Res. Int.* **2022**, *161*, 111842.
(40) Pang, J.; Sha, X.; Chao, Y.; Chen, G.; Han, C.; Zhu, W.; Li, H.; Zhang, Q. Green Aqueous Biphasic Systems Containing Deep Eutectic Solvents and Sodium Salts for the Extraction of Protein. *RSC Adv.* **2017**, *7* (78), 49361−49367.
(41) Yue, J.; Zhu, Z.; Yi, J.; Li, H.; Chen, B.; Rao, J. One-Step Extraction of Oat Protein by Choline Chloride-Alcohol Deep Eutectic Solvents: Role of Chain Length of Dihydric Alcohol. *Food Chem.* **2022**, *376*, 131943.
(42) Delso, I.; Lafuente, C.; Muñoz-Embid, J.; Artal, M. NMR Study of Choline Chloride-Based Deep Eutectic Solvents. *J. Mol. Liq.* **2019**, *290*, 111236.
(43) Khan, A. S.; Ibrahim, T. H.; Jabbar, N. A.; Khamis, M. I.; Nancarrow, P.; Mjalli, F. S. Ionic Liquids and Deep Eutectic Solvents for the Recovery of Phenolic Compounds: Effect of Ionic Liquids Structure and Process Parameters. *RSC Adv.* **2021**, *11* (20), 12398−12422.
(44) Stephens, N. M.; Smith, E. A. Structure of Deep Eutectic Solvents (DESs): What We Know, What We Want to Know, and Why We Need to Know It. *Langmuir* **2022**, *38* (46), 14017−14024.
(45) Aissaoui, T. Novel Contribution to the Chemical Structure of Choline Chloride Based Deep Eutectic Solvents. *Pharm. Anal. Acta* **2015**, *6* (11), 448.
(46) Yue, J.; Zhu, Z.; Yi, J.; Lan, Y.; Chen, B.; Rao, J. Structure and Functionality of Oat Protein Extracted by Choline Chloride−dihydric Alcohol Deep Eutectic Solvent and Its Water Binary Mixtures. *Food Hydrocolloids* **2021**, *112*, 106330.
(47) Ma, Y.; Wang, Q.; Zhu, T. Comparison of Hydrophilic and Hydrophobic Deep Eutectic Solvents for Pretreatment Determination of Sulfonamides from Aqueous Environments. *Anal. Methods* **2019**, *11* (46), 5901−5909.
(48) Gautam, R. K.; Chatterjee, A.; Seth, D. Photophysics Rotational Dynamics and Fluorescence Lifetime Imaging Study of Coumarin Dyes in Deep Eutectic Solvent. *J. Mol. Liq.* **2019**, *280*, 399−409.
(49) Tang, W.; Row, K. H. Design and Evaluation of Polarity Controlled and Recyclable Deep Eutectic Solvent Based Biphasic System for the Polarity Driven Extraction and Separation of Compounds. *J. Clean. Prod.* **2020**, *268*, 122306.
(50) Haque, M. A.; Kaur, P.; Islam, A.; Hassan, M. I. Application of Circular Dichroism Spectroscopy in Studying Protein Folding, Stability, and Interaction. *Adv. Protein Mol. Struct. Biol. Methods* **2022**, 213−224.
(51) Parveen, M.; Uzma; Azam, M.; Azeem, M.; Aslam, A.; Bashir, M.; Alam, M. Catalytic Activity of TiO2 Nanoparticles in Cyclization Reactions for Pyrazolone Formation: DNA Binding Analysis via Spectroscopy, X-Ray Crystallography, and Molecular Docking. *J. Saudi Chem. Soc.* **2024**, *28* (4), 101881.
(52) Dos Santos, N. V.; Saponi, C. F.; Greaves, T. L.; Pereira, J. F. B. Revealing a New Fluorescence Peak of the Enhanced Green Fluorescent Protein Using Three-Dimensional Fluorescence Spectroscopy. *RSC Adv.* **2019**, *9* (40), 22853−22858.
(53) Kadyan, A.; Juneja, S.; Pandey, S. Photophysical Behavior and Fluorescence Quenching of l -Tryptophan in Choline Chloride-Based Deep Eutectic Solvents. *J. Phys. Chem. B* **2019**, *123* (35), 7578−7587.

https://doi.org/10.1021/acsomega.4c09125
ACS Omega 2025, 10, 6839−6856

(54) Han, Q.; Veríssimo, N. V. P.; Bryant, S. J.; Martin, A. V.; Huang, Y.; Pereira, J. F. B.; Santos-Ebinuma, V. C.; Zhai, J.; Bryant, G.; Drummond, C. J.; Greaves, T. L. Scattering Approaches to Unravel Protein Solution Behaviors in Ionic Liquids and Deep Eutectic Solvents: From Basic Principles to Recent Developments. *Adv. Colloid Interface Sci.* **2024**, *331*, 103242.
(55) Florindo, C.; Branco, L. C.; Marrucho, I. M. Development of Hydrophobic Deep Eutectic Solvents for Extraction of Pesticides from Aqueous Environments. *Fluid Phase Equilib.* **2017**, *448*, 135−142.
(56) Makoś, P.; Słupek, E.; Gębicki, J. Hydrophobic Deep Eutectic Solvents in Microextraction Techniques−A Review. *Microchem. J.* **2020**, *152*, 104384.
(57) Liu, J.; Li, X.; Row, K. H. Development of Deep Eutectic Solvents for Sustainable Chemistry. *J. Mol. Liq.* **2022**, *362*, 119654.
(58) Xu, P.; Zheng, G. W.; Zong, M. H.; Li, N.; Lou, W. Y. Recent Progress on Deep Eutectic Solvents in Biocatalysis. *Bioresour. Bioprocess.* **2017**, *4*, 34.
(59) Sanchez-Fernandez, A.; Edler, K. J.; Arnold, T.; Alba Venero, D.; Jackson, A. J. Protein Conformation in Pure and Hydrated Deep Eutectic Solvents. *Phys. Chem. Chem. Phys.* **2017**, *19* (13), 8667−8670.
(60) Li, N.; Wang, Y.; Xu, K.; Huang, Y.; Wen, Q.; Ding, X. Development of Green Betaine-Based Deep Eutectic Solvent Aqueous Two-Phase System for the Extraction of Protein. *Talanta* **2016**, *152*, 23−32.
(61) Lu, W.; Liu, S. Choline Chloride−Based Deep Eutectic Solvents (Ch-DESs) as Promising Green Solvents for Phenolic Compounds Extraction from Bioresources: State-of-the-Art, Prospects, and Challenges. *Biomass Convers. Biorefin.* **2022**, *12* (7), 2949−2962.
(62) Domingues, L.; Duarte, A. R. C.; Jesus, A. R. How Can Deep Eutectic Systems Promote Greener Processes in Medicinal Chemistry and Drug Discovery? *Pharmaceuticals* **2024**, *17* (2), 221.
(63) Shishov, A. Y.; Chislov, M. V.; Nechaeva, D. V.; Moskvin, L. N.; Bulatov, A. V. A New Approach for Microextraction of Non-Steroidal Anti-Inflammatory Drugs from Human Urine Samples Based on in-Situ Deep Eutectic Mixture Formation. *J. Mol. Liq.* **2018**, *272*, 738−745.
(64) Xu, Y.; Wang, Q.; Hou, Y. Efficient Purification of R-Phycoerythrin from Marine Algae (Porphyra Yezoensis) Based on a Deep Eutectic Solvents Aqueous Two-Phase System. *Mar. Drugs* **2020**, *18* (12), 618.
(65) Shishov, A.; Gorbunov, A.; Moskvin, L.; Bulatov, A. Decomposition of Deep Eutectic Solvents Based on Choline Chloride and Phenol in Aqueous Phase. *J. Mol. Liq.* **2020**, *301*, 112380.
(66) Shishov, A.; Dubrovsky, I.; Kirichenko, S.; Bulatov, A. Behavior of Quaternary Ammonium Salts and Terpenoids-Based Deep Eutectic Solvents in Aqueous Phase. *J. Mol. Liq.* **2022**, *347*, 117987.
(67) Zhao, R.-T.; Pei, D.; Yu, P.-L.; Wei, J.-T.; Wang, N.-L.; Di, D. L.; Liu, Y. W. Aqueous Two-Phase Systems Based on Deep Eutectic Solvents and Their Application in Green Separation Processes. *J. Sep. Sci.* **2020**, *43*, 348−359.
(68) Devi, M.; Moral, R.; Thakuria, S.; Mitra, A.; Paul, S. Hydrophobic Deep Eutectic Solvents as Greener Substitutes for Conventional Extraction Media: Examples and Techniques. *ACS Omega* **2023**, *8* (11), 9702−9728.
(69) Santana-Mayor, A.; Rodríguez-Ramos, R.; Herrera-Herrera, A. V.; Socas-Rodríguez, B.; Rodríguez-Delgado, M. A. Deep Eutectic Solvents. The New Generation of Green Solvents in Analytical Chemistry. *TrAC, Trends Anal. Chem.* **2021**, *134*, 116108.
(70) Jiang, Z. M.; Wang, L. J.; Gao, Z.; Zhuang, B.; Yin, Q.; Liu, E. H. Green and Efficient Extraction of Different Types of Bioactive Alkaloids Using Deep Eutectic Solvents. *Microchem. J.* **2019**, *145*, 345−353.

https://doi.org/10.1021/acsomega.4c09125
ACS Omega 2025, 10, 6839−6856